NATIONAL AERONAUTICS AND SPACE ADMINISTRATION

TECHNICAL REPORT
R-120

THEORETICAL DETERMINATION OF THE FORM OF THE HOLLOW PRODUCED IN THE SOLAR CORPUSCULAR STREAM BY INTERACTION WITH THE MAGNETIC DIPOLE FIELD OF THE EARTH

By JOHN R. SPREITER and BENJAMIN R. BRIGGS

1961

TECHNICAL REPORT R-120

THEORETICAL DETERMINATION OF THE FORM OF THE HOLLOW PRODUCED IN THE SOLAR CORPUSCULAR STREAM BY INTERACTION WITH THE MAGNETIC DIPOLE FIELD OF THE EARTH

By JOHN R. SPREITER and BENJAMIN R. BRIGGS

Ames Research Center
Moffett Field, Calif.

TECHNICAL REPORT R-120

THEORETICAL DETERMINATION OF THE FORM OF THE HOLLOW PRODUCED IN THE SOLAR CORPUSCULAR STREAM BY INTERACTION WITH THE MAGNETIC DIPOLE FIELD OF THE EARTH

By John R. Spreiter and Benjamin R. Briggs

SUMMARY

The interaction between a neutral stream of ionized solar corpuscles and a three-dimensional magnetic dipole representing the geomagnetic field is investigated. It is assumed that the stream is confined to the exterior and the magnetic field to the interior of a hollow, the boundary of which is defined by a thin current sheath. An approximate method of solution is applied, and results are presented for the coordinates of the trace of the boundary of the hollow in the meridian plane containing the sun-earth line and the dipole axis for several relative orientations. Results are also presented for the trace in the equatorial plane for the case in which the dipole axis is normal to the sun-earth line. The corresponding problem in two dimensions is also considered, and it is shown that the analogous approximate results are in good agreement with the results indicated by an exact solution of the same basic equations.

INTRODUCTION

The present paper is concerned with the study of the form of the stationary hollow carved out of an extremely rarefied neutral stream of ionized particles flowing at hypersonic speed past the field of a magnetic dipole. Interest in this problem derives from a long series of investigations by Chapman, Ferraro, and others (see refs. 1 and 2 for a résumé) undertaken to explain the connection between solar flares and geomagnetic storms. The broad features that have emerged from these studies and from numerous and diverse observations are that the magnetic variations character- istic of geomagnetic storms are the result of inter-

action between the permanent magnetic field of the earth and streams of neutral ionized gas ejected from the sun. The dimensions of the streams are large compared with the dimensions of the earth, and the gas of which the streams are composed consists mainly of protons and electrons in very nearly equal numbers. The speed of the particles is usually inferred to be of the order of 1000 km/sec from the time lag of about one day between the occurrence of a solar flare and the sudden onset of a geomagnetic storm. The number density of the protons is frequently quoted to be of the order of about 10/cm^3, but is more variable than the velocity and apparently may be as small as 1/cm^3 or as large as 100/cm^3 or 1000/cm^3.

More recent analysis of the properties and behavior of comet tails has led Biermann to advance the idea that there are not only discrete streams of particles ejected from the sun, but also a general radial outflowing of ionized hydrogen from all parts of the sun at all times. This flow has been termed the solar wind and the study of its properties has been the subject of an extensive series of theoretical investigations by Parker and others (see refs. 3 and 4 for a recent account of this work). These studies together with further observational evidence have culminated in the conclusions that the particles constituting the solar wind are mainly protons and electrons in equal number, and that they move outward from the sun as the inevitable hydrodynamic conse- quence of the expansion of the solar corona into interplanetary space. Parker states in reference 4 that at solar minimum, the velocity of expansion may be only 300 km/sec and the number density

1

as low as 20/cm³ at the orbit of the earth. The quiet-day solar wind during the years of solar activity is more intense and Parker goes on to suggest that the velocity and number density may exceed 500 km/sec and 100/cm³ at such times.

The close similarity between the properties of the solar wind and the corpuscular-streams associated with geomagnetic storms is obvious. It follows that many of the phenomena associated with the interaction of the solar wind and the geomagnetic field are essentially the same as those associated with the steady state established within a few minutes after the sudden commencement of a geomagnetic storm when the earth becomes fully immersed in the solar corpuscular stream. It has been suggested by Zhigulev and Romishevskii (ref. 5), Dungey (ref. 6), and Obayashi and Hakura (ref. 7) that a closely related situation also occurs even in the absence of the solar wind or corpuscular streams as a result of the earth's motion in its orbit through an ionized medium. It is not certain, however, that the associated phenomena are analogous in all details. The reason is that the orbital velocity of the earth is an order of magnitude smaller than the velocities quoted above for the interplanetary gas flows, and the effects resulting from the random motion of the particles, which are customarily neglected in the study of these problems, would be expected to be relatively greater.

Although the fundamental concepts and equations governing the interaction between a neutral stream of ionized solar corpuscles and a three-dimensional magnetic dipole representing the permanent geomagnetic field have been established for many years, the solution of the resulting problem has proved to be a difficult task. Most investigations of this problem have involved a reduction in the number of dimensions, but Beard has recently presented an analysis in reference 8 in which the full three-dimensional character of the problem is retained throughout. Simplification is achieved by relinquishing one of the boundary conditions and replacing it by an approximate relation that is exact for the related one-dimensional flow. In this way, Beard is enabled to derive a rather lengthy nonlinear partial differential equation for the coordinates of the surface bounding the hollow. He then proceeds to determine the solution in certain regions

where marked simplification occurs by reason of symmetry. Results are thus given for the coordinates of the surface in the equatorial plane, and also in the vicinity of the meridian plane containing the dipole axis and the velocity vector of the undisturbed corpuscular stream for the special case in which these two directions are perpendicular.

Examination of the results for the meridian plane reveals, however, that they do not all satisfy the governing differential equation developed in the main body of the analysis. The principal steps of Beard's analysis are therefore reviewed in the present paper preliminary to the presentation of the new results. Ferraro has, in addition, presented some comments in reference 9 and suggested that it would be better, and no more difficult, to use a slightly different approximate relation. This suggestion has accordingly been incorporated into the present analysis, but it is a simple matter to recover the equations of Beard from the equations given herein, if desired.

The principal contribution of the present investigation is, however, the determination of the trace of the boundary of the hollow in the meridian plane containing the dipole axis and the velocity vector of the incident stream for several cases in which these two directions are not perpendicular.

Since two-dimensional models have played an important role in many previous discussions of the present and related geophysical problems, the equations for the corresponding two-dimensional problem are also introduced and the approximate solution is presented. It is found that the form of the hollow is similar in most, but not all respects, to that found for the three-dimensional model. An indication of the quality of the results to be expected from the approximate solutions is provided by comparison of the approximate results obtained for the form of the hollow with the exact results for the two-dimensional model given by Zhigulev and Romishevskii (ref. 5), Hurley (ref. 10), and Dungey (ref 6). It is shown that the form of the boundary indicated by the approximate solution is in good agreement with that indicated by the exact solution.

FUNDAMENTAL ASSUMPTIONS AND EQUATIONS

The fundamental assumptions and equations of the present analysis are based on the results of previous investigations of Beard (ref. 8), Ferraro

(refs. 9 and 11), and Dungey (ref. 12), which are, in turn based on a long series of investigations by Chapman and Ferraro, and others that have been summarized recently in references 1 and 2. It is assumed in these and related studies that a steady neutral ionized corpuscular stream flows radially outward from the sun. The presence of the geomagnetic field has the effect of carving a hollow out of the stream. The hollow is bounded by a thin current sheath, which has the property of confining the corpuscular stream to the exterior, and the geomagnetic field to the interior of the hollow.

Dungey (ref. 12) has investigated in detail the conditions that prevail, for the steady state, at the surface of the hollow where the aerodynamic pressure of the deflected stream is balanced by the magnetic and electrical forces on the charged particles. It is found that the particles of the corpuscular stream move in straight lines up to the boundary of the hollow where they are, in effect, specularly reflected and returned to the stream with a direction of motion different from that which they possessed in the incident stream. In so doing they exert an aerodynamic pressure $2mnr^2\cos^2\psi$ on any element of the boundary for which $\cos \psi \leq 0$. The quantities m, n, and r represent the mass, number density, and velocity of the positive ions in the undisturbed incident stream and ψ represents the angle which the direction of the undisturbed motion of the particles makes with the outward normal to the surface at the point of impact. An element of the surface that fails to comply with the condition that cos

Element of boundary
of hollow, $F(r, \theta, \phi)$
= constant

$\hat{n}_s$, outward normal to
boundary of hollow

z

θ

M_p

y

ϕ

λ

v

x

FIGURE 1. View of coordinate system.

$\psi \leq 0$ is shielded from the stream and experiences no aerodynamic pressure.

Dungey proceeds to show that the aerodynamic pressure is balanced by the magnetic pressure $H_s^2/8\pi$ where H_s is the total (tangential) magnetic field at the surface of the hollow. These considerations lead to the following relation which must be satisfied at the boundary of the hollow:

$$H_s^2/8\pi = 2mnr^2 \cos^2\psi \qquad (1)$$

With m, n, and r expressed in c.g.s. units, H_s is expressed in gauss.

The total magnetic field $\mathbf{H}$ in the interior of the hollow is the sum of the permanent magnetic field $\mathbf{H}_p$ and the induced magnetic field $\mathbf{H}'$ due to the currents in the stream surface. This field depends on the shape of the hollow, and its properties are described by the solution of the magnetic field equations

$$\text{div } \mathbf{H} = 0, \text{ curl } \mathbf{H} = 0 \qquad (2)$$

which satisfies the boundary conditions that the normal component of $\mathbf{H}$ vanish and the tangential component of $\mathbf{H}$ be given by equation (1) at the surface of the hollow. It is also necessary that the solution possess the appropriate singularities in the interior of the hollow that are required to represent the magnetic field of the earth and any exterior current systems that may be present. These will be considered to be represented by a single magnetic dipole. Thus, $\mathbf{H}_p$ for the three-dimensional case is given by

$$\mathbf{H}_p = -(M_p/r^3)\,(\hat{\theta}\sin\theta + \hat{r}2\cos\theta) \qquad (3)$$

where the coordinate system is fixed with respect to the dipole as illustrated in figure 1, $\hat{\theta}$ and $\hat{r}$ are unit vectors in the direction of increasing θ and r, and the magnetic moment of the dipole is given by $M_p = a^3 H_{p_0}$, where a represents the radius of the earth and H_{p_0} represents the intensity of the geomagnetic field at the magnetic equator. The corresponding expression for the permanent magnetic field in the two-dimensional case is

$$\mathbf{H}_{p_2} = -(M_{p_2}/r^2)\,(\hat{\theta}\sin\theta + \hat{r}\cos\theta) \qquad (4)$$

where the magnetic moment of the two-dimensional dipole is given by $M_{p_2} = a^2 H_{p_0}$, and the subscript 2 is used where necessary to denote
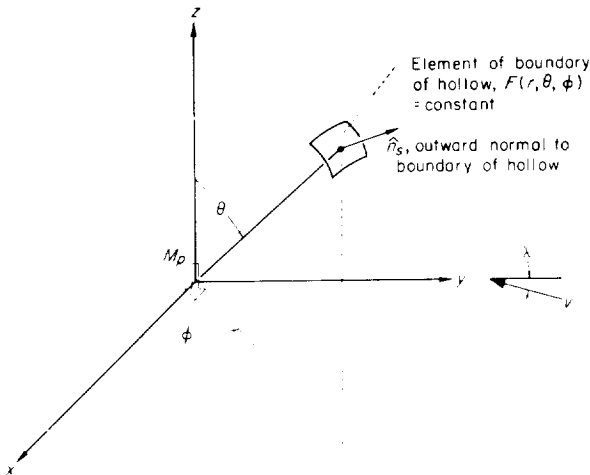
the values of the indicated quantities that are associated with the two-dimensional problem.

It is a property of the above equations that **H** cannot vanish over any region of finite extent in the interior of the hollow. It follows that the boundary of the hollow must be of such form that $\cos \psi \leq 0$ everywhere with zero values occurring only at isolated points or lines. This condition together with the above equations suffices to specify completely the form for the boundary of the hollow and the properties of the magnetic field contained therein.

Comparison of the mathematical formulation of the problem summarized above with that derived in an earlier detailed study by Ferraro given in reference 11 reveals one difference. It is that Ferraro arrives at the following expression in place of equation (1):

$$H_s^2/8\pi = mnr^2 \cos^2 \psi \qquad (5)$$

This result indicates that only half the aerodynamic pressure is balanced by the magnetic pressure. Ferraro states that this implies that the other half is balanced by a retarding electrostatic field associated with a slight charge separation in the vicinity of the boundary. Such a separation occurs as a consequence of the fact that the more massive ions penetrate slightly deeper into the boundary than the electrons.

The resultant effect of using equation (5) rather than (1) is that all linear dimensions of the hollow are larger by a factor of $2^{1/6}$ for the three-dimensional case and $2^{1/4}$ for the two-dimensional case. Further examination of the literature reveals that equations (1) and (5) have both been used in recent studies. Equation (1) has been used, for instance, in references 5, 8, 10, and 12 by Zhigulev and Romishevskii, Beard, Hurley, and Dungey, respectively. On the other hand, recent studies by Ferraro (refs. 2 and 9), as well as those of Chapman (ref. 1), Obayashi and Hakura (ref. 7), Piddington (ref. 13), and the present authors (ref. 14) are all based on equation (5).

The choice of equation (1) or (5) to represent the conditions at the boundary of the geomagnetic field is obviously a matter that requires clarification. It is fortunate, therefore, that the two principal derivations of these equations, namely

those given by Dungey in reference 12 and by Ferraro in reference 11, are based on essentially the same fundamental concepts and equations. The analysis given by Ferraro is much longer, however, because it includes consideration of the unsteady case, whereas that given by Dungey is confined to the steady-state case. It appears, in fact, that the slightly different objectives in the two derivations account for the difference in the final result.

Thus, Ferraro is concerned principally with the first phase of a geomagnetic storm during which it is considered that a neutral ionized cloud of finite extent advances toward the earth and compresses the magnetic field. It is assumed, in the analysis, that the density of the stream just inside the leading face of the cloud is not increased appreciably by the presence of overtaken or rebounding particles. The actual increase is not calculated, but it is concluded on the basis of examination of conditions that prevail in the very early stages of the interaction when the cloud is very distant from the earth that the increase is indeed small. It is then shown that these arguments lead to equation (5). This result is then applied in the discussion of not only the initial phase of the unsteady case but also the final steady-state case in which the particles are, in effect, specularly reflected from the boundary of the geomagnetic field.

Dungey concentrates, on the other hand, on an analysis of the conditions that prevail when the earth is deeply immersed in a neutral ionized cloud and a steady state has been established. Consideration is given to the increase in the density of the stream just outside the boundary of the magnetic field due to the presence of rebounding particles. Since the number of rebounding particles is just equal, in the steady state, to the number of particles in the incident stream at the same point, the density of the stream in the vicinity of the boundary is just twice that associated with the incident stream alone. These considerations, when applied to the inhomogeneous Maxwell's equations, lead to the factor 8 in the right-hand members of equation (8.7) and (8.8) of Dungey's analysis compared with the factor 4 in the right-hand members of equations (16) and (21) of Ferraro's analysis, and account ultimately for the factor 2 in the right-

hand member of equation (1) compared with unity in equation (5). The final conclusion is that the relation given by equation (1) is the appropriate condition to apply at the boundary of the geomagnetic field for analysis of steady-state problems. Ferraro has indicated in private correspondence with the authors that he concurs with this conclusion.

Attention is drawn to the fact that Dungey appears to use equation (5) rather than (1) in his more recent work given in reference 6. There is a slight ambiguity in the definition of the number density n, however, and it appears upon closer examination that this quantity refers to the sum of the incident and reflected ions rather than the number of ions in the incident stream alone, as in his previous work. With this interpretation, the relation employed in reference 6 is equivalent to equation (1) rather than (5).

THREE-DIMENSIONAL PROBLEM

DERIVATION OF AN APPROXIMATE DIFFERENTIAL EQUATION FOR THE COORDINATES OF THE BOUNDARY OF THE HOLLOW

An exact solution for the form of the boundary of the hollow for the two-dimensional case has been given recently by Zhigulev and Romishevskii (ref. 5), Hurley (ref. 10), and Dungey (ref. 6), but it was necessary for Beard to resort to approximate methods in reference 8 to obtain comparable results for the physically realistic three-dimensional case. The essential concept that leads to the simplification achieved by Beard is that the condition that the normal component of **H** vanish at the boundary of the hollow is relinquished and replaced by the approximate condition that H_s is equal to twice the tangential component of the permanent magnetic field $\mathbf{H}_p$ at the same point.

Ferraro has subsequently presented some comments in reference 9 regarding this approximation and suggested that it would be better to replace the factor 2 by 2f where f is a constant, the value for which is to be determined at the end of the calculation by matching conditions at some particularly significant point. He presents a simple illustrative two-dimensional example involving flow past a current-bearing wire and shows that a reasonable procedure for the estimation of f leads to the value 0.68 for that particular case. It will

be seen subsequently herein that the corresponding value for f increases to about 0.913 when flow past a two-dimensional dipole is considered. It will also been seen that introduction of a constant factor f into the analysis affects only the size and not the form of the hollow. The effect is, moreover, of only moderate importance in the three-dimensional case since the linear dimensions of the hollow are proportional to the cube root of f, and it is anticipated that values for f will be only slightly different from unity.

The mathematical implementation of the above considerations requires the determination of the appropriate expression for the component of the permanent magnetic field that lies in the surface of the hollow. This has been accomplished, except for omission of sign, by Beard and the result having positive sense in the direction of increasing θ is given by

$$\hat{p} \cdot \mathbf{H}_p = -(b'Mp/r^3)[\sin \theta + (2/r)(\partial r/\partial \theta) \cos \theta] \quad (6)$$

where

$$b' = [1 + (1/r^2)(\partial r/\partial \theta)^2]^{-1/2} \quad (7)$$

and $\hat{p} = k(\hat{\varphi} \times \hat{n}_s)$ is a unit vector in the direction of the line of intersection of the surface of the hollow and a plane $\varphi = \text{const}$, $\hat{n}_s$ is a unit vector in the direction of the outward normal to the surface, k is a normalizing factor, and the quantities r and θ now refer to the coordinates of the surface of the hollow. Equation (6), together with the assumption that

$$H_s = 2f(\hat{p} \cdot \mathbf{H}_p) \quad (8)$$

suffices to provide the relation necessary to express the left-hand side of equation (1) in terms of the coordinates of the surface of the hollow and the dipole moment of the permanent magnetic field.

It is also necessary to determine the appropriate expression for the right-hand side of equation (1) in terms of the coordinates of the boundary of the hollow. The essential part of this term is the quantity $\cos \psi$, which Beard has shown can be written as follows in terms of the equation $F(r, \theta, \varphi) = \text{const}$ defining the boundary, and the

angle λ between the direction of the incident stream and the normal to the axis of the dipole.

$$\cos \psi = \hat{n}_x \cdot \mathbf{v} = -a \left[\frac{\partial F'}{\partial r} (\sin \varphi \sin \theta \cos \lambda - \cos \theta \sin \lambda) \right.$$

$$+ \frac{1}{r} \frac{\partial F'}{\partial \theta} (\sin \varphi \cos \theta \cos \lambda + \sin \theta \sin \lambda)$$

$$\left. + \frac{1}{r \sin \theta} \frac{\partial F'}{\partial \varphi} \cos \varphi \cos \lambda \right] \quad (9)$$

where

$$a = \left[\left(\frac{\partial F'}{\partial r} \right)^2 + \frac{1}{r^2} \left(\frac{\partial F'}{\partial \theta} \right)^2 + \frac{1}{r^2 \sin^2 \theta} \left(\frac{\partial F'}{\partial \varphi} \right)^2 \right]^{-1/2} \quad (10)$$

and

$$dF = \frac{\partial F'}{\partial r} dr + \frac{\partial F'}{\partial \theta} d\theta + \frac{\partial F'}{\partial \varphi} d\varphi = 0 \quad (11)$$

Combination of equations (1) and (6) through (11) together with the dimensionless radius $\rho = r/r_0$ where

$$r_0 = \left(\frac{4f^2 M_p^2}{16\pi m n v^2} \right)^{1/6} = a \left(\frac{4f^2 H_{p_0}^2}{16\pi m n v^2} \right)^{1/6} \quad (12)$$

leads to the following differential equation for the radial coordinate ρ of the boundary of the hollow expressed as a function of the angular coordinates θ and φ

$$\pm \frac{b'}{\rho^3} \left(\sin \theta + \frac{2}{\rho} \frac{\partial \rho}{\partial \theta} \cos \theta \right)$$

$$= a' \left[(\sin \varphi \sin \theta \cos \lambda - \cos \theta \sin \lambda) \right.$$

$$- \frac{1}{\rho} \frac{\partial \rho}{\partial \theta} (\sin \varphi \cos \theta \cos \lambda + \sin \theta \sin \lambda)$$

$$\left. - \frac{1}{\rho \sin \theta} \frac{\partial \rho}{\partial \varphi} \cos \varphi \cos \lambda \right] \quad (13)$$

in which the normalizing factor a' is defined by

$$a' = [1 + (1/\rho^2)(\partial \rho/\partial \theta)^2 + (1/\rho^2 \sin^2 \theta)(\partial \rho/\partial \varphi)^2]^{-1/2} \quad (14)$$

and b' is defined by the relation given in equation (7) with ρ written in place of r. It follows from the dimensionless character of this equation that variations in the density and velocity of the undisturbed corpuscular stream, and also in the value selected for the factor f affect the size but not the shape of the hollow. These quantities enter

only into the definition of r_0, which will be shown in the next section to represent the distance of the apex of the hollow from the dipole singularity for the special case in which λ is zero.

The right-hand side of equation (13) is equal to $-\cos \psi$ and is therefore positive everywhere on the surface of the hollow. The sign of the quantity within the parentheses in the left-hand side may be positive or negative, however, depending upon whether the component of the permanent magnetic field that lies in the surface of the hollow is oriented in the general direction of decreasing or increasing θ. It is evident that both cases occur in the desired solution.

SOLUTION FOR MERIDIAN PLANE CONTAINING DIPOLE AXIS AND SUN-EARTH LINE

The solution of equation (13) appears to be a complex problem, but great simplification occurs if attention is confined to the determination of the trace of the boundary of the hollow in the meridian plane containing the dipole axis and the sun-earth line, that is, the plane along which $\varphi = \pm \pi/2$. Along this plane $\partial r/\partial \varphi$ vanishes by reason of symmetry and equation (13) reduces to

$$\pm \frac{1}{\rho^3} \left(\sin \theta + \frac{2}{\rho} \frac{d\rho}{d\theta} \cos \theta \right) = \sin \theta \cos \lambda \sin \left(\pm \frac{\pi}{2} \right)$$

$$- \cos \theta \sin \lambda - \frac{1}{\rho} \frac{d\rho}{d\theta} \left[\cos \theta \cos \lambda \sin \left(\pm \frac{\pi}{2} \right) \right.$$

$$\left. + \sin \theta \sin \lambda \right] \quad (15)$$

or, solving for $d\rho/d\theta$, to

$$\frac{d\rho}{d\theta} = (\rho \tan \theta) \left\{ \frac{\rho^3 [\cos \lambda \sin (\pm \pi/2) - \cot \theta \sin \lambda] \mp 1}{\rho^3 [\cos \lambda \sin (\pm \pi/2) + \tan \theta \sin \lambda] \pm 2} \right\} \quad (16)$$

where the sense of the plus and minus signs has been retained to be the same as in equation (13) by writing $\sin (\pm \pi/2)$ in the right-hand members. This result agrees with that given by Beard for $\lambda = 0$ for $\varphi = \pi/2$. It differs, however, in the overall sign of the right-hand side from the corresponding result indicated by Beard's equation (36) for the special case in which $\lambda = 0$, $\varphi = -\pi/2$, and $\rho \leq 2^{1/3}$ in the notation of the present paper.

It is apparent that equations (15) and (16) have two families of solutions for any given λ, depending upon the choice of the upper or lower signs. It is

convenient for the discussion of the solutions to drop the consistent use of the plus and minus sign employed to this point and consider the two rearranged families of solutions associated with the following equation equivalent to equation (16):

$$\frac{d\rho}{d\theta} = \rho \frac{\rho^3 \sin [\theta - \lambda \sin (\pm \pi/2)] \mp \sin \theta}{\rho^3 \cos [\theta - \lambda \sin (\pm \pi/2)] \pm 2 \cos \theta} \quad (17)$$

The solutions are given by

$$\rho \cos \left[\theta - \lambda \sin \left(\pm \frac{\pi}{2}\right)\right] \mp \frac{1}{\rho^2} \cos \theta = K \quad (18)$$

where K is an arbitrary constant of integration. The above equations apply for both positive and negative values for λ, but it is convenient to restrict attention in the remainder of the discussion to positive λ. The corresponding results for negative values for λ can be obtained readily by symmetry from the results for an equal positive angle.

The evaluation of K cannot be achieved directly since there is no point on the boundary for which the coordinates ρ and θ are known from a priori considerations. Examination of the properties of the integral curves defined by equation (18) discloses, however, that only one of the many alternative solutions satisfies the condition that the hollow extends a finite distance from the earth in the direction of the sun, and that the lateral dimensions of the hollow increase steadily with distance downstream from the apex so that $\cos \psi \leq 0$ at all points. This statement is illustrated most readily for the simplified form of equation (18) that results for $\lambda = 0$, and that case will be considered first.

Results for $\lambda = 0$. The solutions given by equation (18) reduce for the case of $\lambda = 0$ to

$$\zeta = \frac{z}{r_0} = \rho \cos \theta \mp \frac{K \rho^3}{\rho^3 \mp 1} \quad (19)$$

Plots of the integral curves are shown in figure 2 for several values for K. It should be observed that of all the integral curves, only the one shown on part (a) which describes the unit circle

$$\rho = 1 \quad (20)$$

intersects the sun-earth line at a distance from the origin that is neither zero nor infinite. This solution, which is obtained from equation (19)

by using the minus sign and equating K to zero, is, therefore, the only one that can represent the form of the hollow in the vicinity of the apex. It is evident, however, that this curve cannot represent the form of the hollow for $\varphi = -\pi/2$ since it turns away from the direction of the corpuscular stream over the pole and fails to satisfy the condition that $\cos \psi \leq 0$.

An interesting development enters at this point since inspection of the integral curves shown in part (b) of figure 2 reveals that the only other integral curve that passes through the point $\rho = 1$ over the pole also fails to satisfy the condition that $\cos \psi \leq 0$. Further inspection of the two sets of integral curves reveals, however, that there is one, and only one, integral curve that can be joined to the upper half of the unit circle at some point in in the quadrant in which $\varphi = \pi/2$, and that extends to infinity in the downstream direction with $\cos \psi \leq 0$ at all points. It is the integral curve shown on part (b) of figure 2 for $K = 3/2^{2/3} \approx 1.890$, that is, that defined by

$$\zeta = \rho \cos \theta = \frac{3}{2^{2/3}} \frac{\rho^3}{\rho^3 + 1} \approx 1.890 \frac{\rho^3}{\rho^3 + 1} \quad (21)$$

The two curves meet at the point on the unit circle having an angular coordinate θ_{cr} given by

$$\theta_{cr} = \cos^{-1}\left(\frac{3}{4}\right)(2^{1/3}) = \frac{1}{3} \text{ radian} \approx 19.1° \quad (22)$$

These two curves together with a third curve joined to the lower half of the unit circle in a corresponding manner determine the trace of the boundary of the hollow in the meridian plane containing the sun-earth line and the dipole axis for the case in which these two directions are perpendicular. A plot of the result is shown in figure 3.

It is important to observe that the curves selected to define the boundary of the hollow are portions of the integral curves shown in figure 2 that possess the property of crossing. Points at which the integral curves cross are denoted as singular points, and are determined by the condition that the numerator and denominator of the right-hand member of equation (17) vanish simultaneously. Although the positions of the singular points are different for $\lambda \neq 0$, it will be seen in the next section that the integral curves associated with the singular points continue to play an
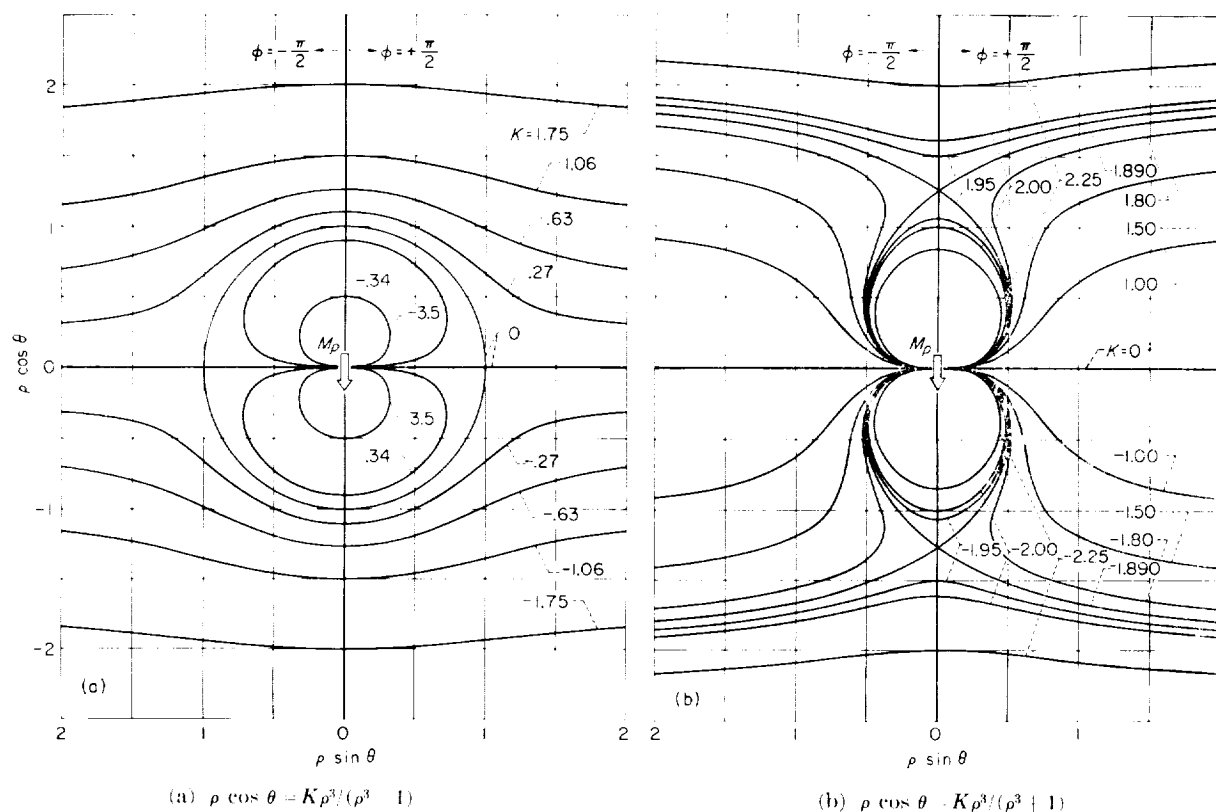
(a) $\rho \cos \theta = K\rho^3/(\rho^3 - 1)$

(b) $\rho \cos \theta = K\rho^3/(\rho^3 + 1)$

FIGURE 2.—Integral curves defined by equation (19).

analogous role in the determination of the solution, although a modification enters when λ exceeds a certain value.

The points at which the front and rear portions of the boundary join are also of particular significance. The segments of the boundary on opposite sides of these points arise mathematically from solutions of equation (17) with alternate choice of upper and lower signs. Physically, this situation indicates, considering the relation between the role of the signs in equations (15) and (17), that the magnetic field lines, and hence also the currents in the current sheath, are directed in opposite directions at points on the boundary on the two sides of these points. These points thus correspond to the neutral points at which the magnetic lines defining the boundary of the hollow meet, turn abruptly, and extend to the earth. The intersection of these lines and the earth's surface defines a pair of isolated points in the vicinity of the geomagnetic poles through which pass all the field lines that lie in and define the boundary of the hollow. These points are of special significance because they define the geo-

graphical areas into which charged particles initially trapped in the vicinity of the hollow can precipitate.

An important property of the boundary at the neutral points is lost in the present solutions as a consequence of the introduction of the approximation that H_s is equal to $2f$ times the tangential component of the permanent magnetic field. It is that $\cos \psi$ must vanish at the neutral points. That this condition must apply follows from consideration of equation (1) together with the fact that exact solutions of equation (2) and the stated boundary conditions must indicate zero field strength at a point of bifurcation of field lines such as occurs at a neutral point. The inability of the present results to display this property clearly represents at least a local failure of the approximation. It is anticipated, on the basis of comparisons of exact and approximate solutions of the corresponding two-dimensional problem shown subsequently herein, that the effects of this failure of the approximate solutions are not global in character, but are confined es-
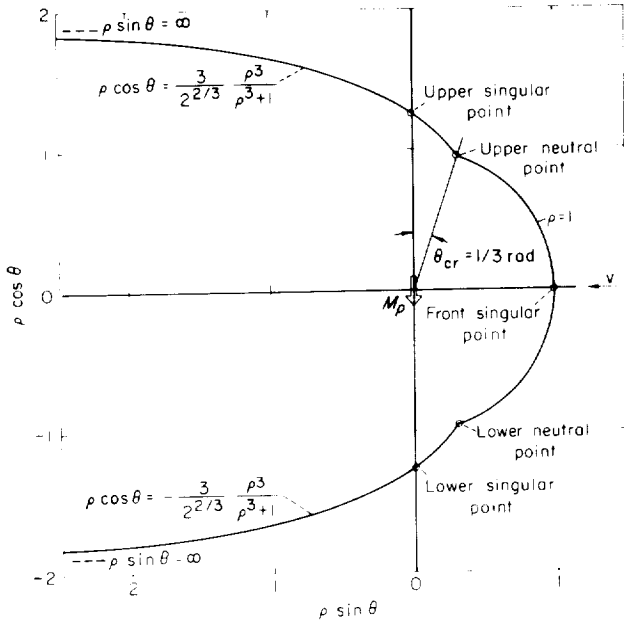
FIGURE 3. Form of the boundary of the hollow in the meridian plane containing the dipole axis and the sun-earth line; $\lambda = 0$.

sentially to small regions in the immediate vicinity of the neutral points.

It is evident from the foregoing results that the form of the hollow is independent of the values for the velocity r and number density n of the corpuscular stream, but that the size depends on these quantities through the parameter r_0 defined by equation (12). The relation between these quantities is illustrated in figure 4 for two representative values for f, namely 1 and 3/4. Considerable uncertainty exists at the present time in the selection of appropriate values for r and n, but values frequently quoted are in the range from 300 to 1500 km/sec for r, and 1 to 100 or more for n. A representative set of values for r, n, and f are 500 km/sec, 10, and 1, for which it can be seen from figures 3 and 4 that the minimum distance to the boundary is about 7.6 earth radii. A plot of the upper half of the boundary of the hollow is shown for this case in figure 5.

Also shown in figure 5 are the corresponding results indicated by Beard in reference 8. The two results agree over the circular portion of the boundary nearest the sun, but not over the portion of the boundary extending from infinity on the night side to a colatitude of 19.1° on the day side.

Beard has informed the present authors privately that these differences result from the fact that the present authors base their analysis on the approximation given by equation (8) at all points on the boundary whereas he uses another approximation in the vicinity of the points over the poles.

Results for arbitrary λ.—The evaluation of the integration constant K to be used in equation (18) to determine the boundary of the hollow for arbitrary λ requires consideration of the coordinates ρ_S and θ_S of the singular points of equation (17). They are determined by equating the numerator and denominator of the right-hand member of equation (17) to zero and solving the two resulting algebraic equations simultaneously. This procedure leads directly to the relation

$$\tan \theta_S + 2 \tan [\theta_S - \lambda \sin (\pm \pi/2)] = 0 \qquad (23)$$
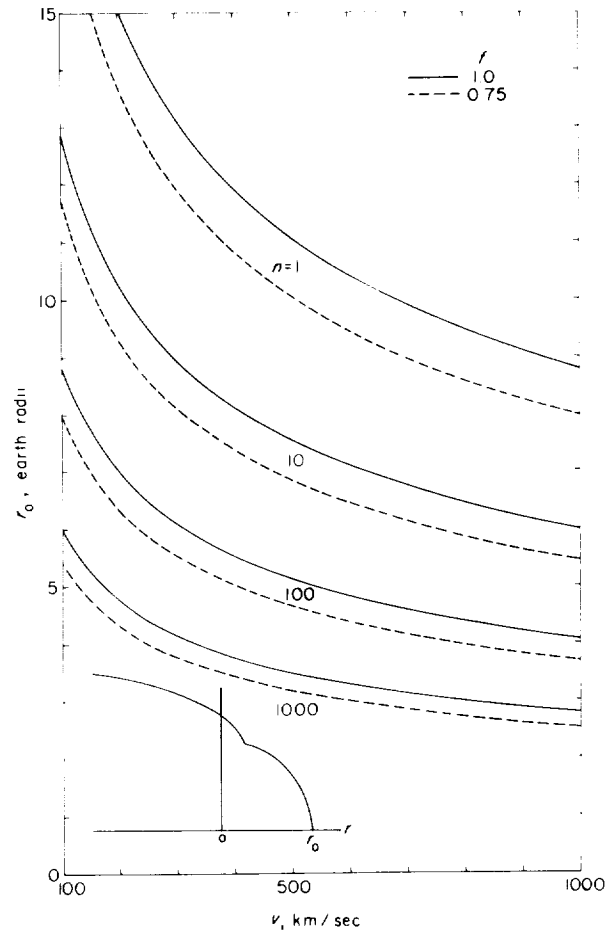

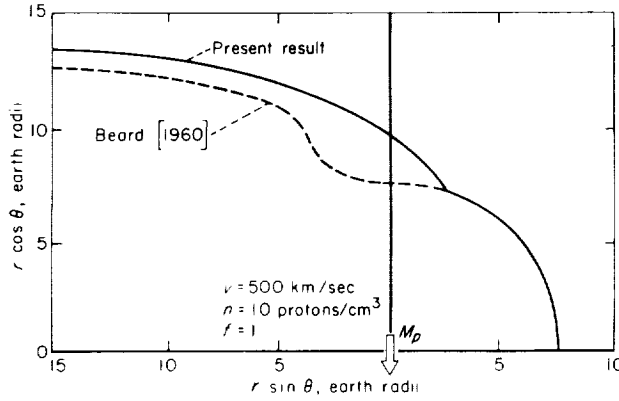FIGURE 4. Values for r_0 for various velocities and number densities of the corpuscular stream.

FIGURE 5. Comparison of present results and those given by Beard in reference 8 for the trace of the boundary of the hollow in the meridian plane containing the dipole axis and the sun-earth line: $\lambda = 0$, $v = 500$ km/sec, $n = 10$ protons/cm³, and $f = 1$.

which can be solved to yield the following expression for the angular coordinates of the singular points:

$$\tan \theta_S = -\frac{3}{2}\left[\cot \lambda \sin\left(\pm\frac{\pi}{2}\right)\right]\left(1 \pm \sqrt{1 + \frac{8}{9}\tan^2\lambda}\right) \tag{24}$$

The associated expression for the radial coordinates of the singular points follows immediately and is

$$\rho_S = \left[\frac{1}{2}\left(\mp \cos\lambda + \sqrt{9 - \sin^2\lambda}\right)\right]^{1/3} \tag{25}$$

with the convention regarding the use of the upper and lower signs in equations (24) and (25) remaining the same as for equations (17) and (18). There are thus two singularities in the front half plane for which $\varphi = \pi/2$ and two in the rear half plane for which $\varphi = -\pi/2$.

It is of interest to examine the approximate expressions for the coordinates that are obtained for small λ, even though the exact expressions are used in the calculation of the numerical results to be presented subsequently herein. They are as follows for the two singularities situated in the front half plane:

$$\theta_{S_F} \approx \frac{\pi}{2} + \frac{\lambda}{3}, \qquad \rho_{S_F} \approx 1 + \frac{\lambda^2}{18} \tag{26}$$

and

$$\theta_{S_U} \approx \frac{2\lambda}{3}, \qquad \rho_{S_U} \approx 2^{1/3}\left(1 - \frac{\lambda^2}{18}\right) \tag{27}$$

The subscripts F and U refer to the singularities associated with the front and upper rear portions of the boundary, respectively. The corresponding expressions for the remaining singularities situated in the rear half plane are

$$\theta_{S_L} \approx \pi - \frac{2\lambda}{3}, \qquad \rho_{S_L} \approx 2^{1/3}\left(1 - \frac{\lambda^2}{18}\right) \tag{28}$$

and

$$\theta_{S_R} \approx \frac{\pi}{2} - \frac{\lambda}{3}, \qquad \rho_{S_R} \approx 1 + \frac{\lambda^2}{18} \tag{29}$$

The subscript L refers to the singularity associated with the lower rear portion of the boundary and the subscript R refers to a singularity that has physical meaning only if the direction of the incident stream is reversed.

The values for K_S associated with the integral curves that pass through the singular points can be determined from the general solution given by equation (18) upon substitution of θ_S and ρ_S for θ and ρ, thus

$$K_S = \rho_S \cos\left[\theta_S - \lambda \sin\left(\pm\frac{\pi}{2}\right)\right] \mp \frac{1}{\rho_S{}^2}\cos\theta_S \tag{30}$$

A somewhat simpler relation that does not explicitly involve λ can be obtained by combination with the equation obtained by equating the denominator of equation (17) to zero, and introducing a similar substitution for θ and ρ. The resulting expressions for the values for K_S for the three singular points of interest are

$$K_{S_F} = -\frac{3\cos\theta_{S_F}}{\rho_{S_F}{}^2}, \qquad K_{S_U} = \frac{3\cos\theta_{S_U}}{\rho_{S_U}{}^2},$$

$$K_{S_L} = \frac{3\cos\theta_{S_L}}{\rho_{S_L}{}^2} \tag{31}$$

A list of values for θ_S, ρ_S, and K_S for various λ is given in table I. The values for θ_S and λ are given in degrees.

Further discussion of the solution is facilitated by inspection of the two sets of integral curves defined by equation (18) shown in figure 6 for the special case in which λ is 30°. The curves associated with the upper signs of equation (18) are shown in part (a), and those associated with the lower signs are in part (b). The locations of the four singular points are indicated on the curves and their significance as points where the

(a) $\rho \cos\left[\theta - \lambda \sin\left(\pm\dfrac{\pi}{2}\right)\right] - \dfrac{1}{\rho^2}\cos\theta = K$

(b) $\rho \cos\left[\theta - \lambda \sin\left(\pm\dfrac{\pi}{2}\right)\right] + \dfrac{1}{\rho^2}\cos\theta = K$
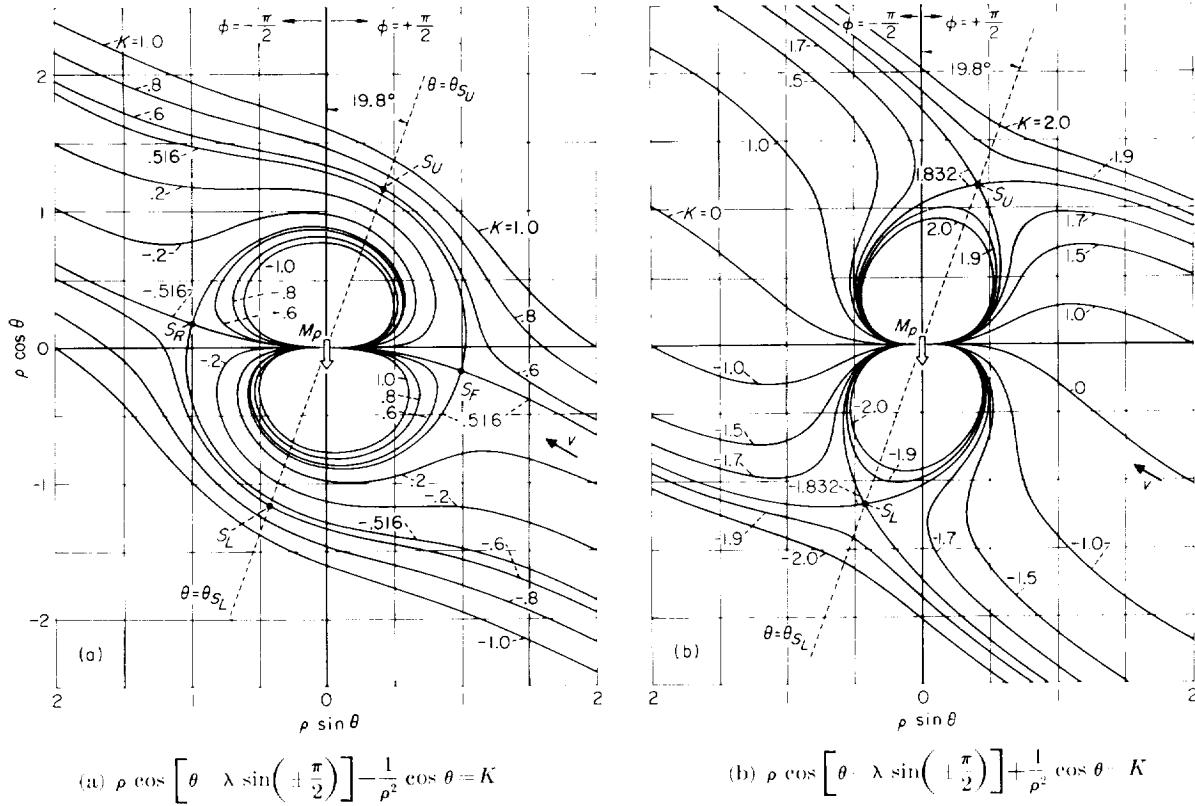
FIGURE 6.— Integral curves defined by equation (18); $\lambda = 30°$.

integral curves cross is apparent. The line described by equating θ to θ_{S_U} and θ_{S_L} has additional significance since all the integral curves, except those shown on figure 6(b) that pass through the upper and lower singular points, are parallel to the direction of the corpuscular stream at the point where they intersect this line. This result can be established analytically from consideration of equations (17) and (18) together with the following relation, which is equivalent to $\cos\psi = 0$,

$$\frac{d\{\rho\cos[\theta - \lambda\sin(\pm\pi/2)]\}}{d\theta} = 0 \qquad (32)$$

A dashed line indicating the locus of the points defined by $\theta = \theta_{S_U}$ and $\theta = \theta_{S_L}$ is therefore included in both parts of figure 6.

The selection of the appropriate integral curves to represent the boundary of the hollow proceeds in a manner that is completely analogous to that described in the preceding section for the case in which $\lambda = 0$. Thus, of all the integral curves, only the one shown on part (a) that passes

through the front singular point and has the value K_{S_F} for K can be used to represent the boundary of the hollow in the vicinity of the apex. It is evident, however, that this curve cannot represent the form of the entire hollow since it turns away from the direction of the corpuscular stream and fails to satisfy the condition that $\cos\psi \leq 0$ at stations farther from the sun than the line defined by $\theta = \theta_{S_U}$ and $\theta = \theta_{S_L}$. The remainder of the boundary must therefore be constructed from portions of the integral curves shown on figure 6(b). Examination of these results reveals, however, that the integral curves which can be joined at the points where $\cos\psi = 0$ to the curve describing the forepart of the hollow neither extend to infinity in the downstream direction nor satisfy the condition that $\cos\psi \leq 0$ in the region of interest. Further examination reveals that there is one and only one pair of integral curves that satisfies these conditions and that can be joined to the curve representing the forepart of the hollow anywhere upstream of the points at which $\cos\psi = 0$. It is the pair of integral

FIGURE 7.—Form of the boundary of the hollow in the meridian plane containing the dipole axis and the sun-earth line; $0° \leq \lambda \leq 35°$.

curves having values for K of K_{SU} and K_{SL} that pass through the upper and lower singular points. These three segments of integral curves thus define the trace of the boundary of the hollow

in the meridian plane containing the dipole axis and the sun-earth line for the case in which $\lambda = 30°$.

The procedure described above has been used to calculate the form of the boundary of the

hollow for several values for λ between $0°$ and $35°$. The numerical values for ρ are listed as a function of θ for intervals of $5°$ in θ and λ in table II, and illustrated graphically in figure 7. The coordinates of the upper and lower neutral points at which the front and rear portions of the boundary join are also of interest and the numerical values are listed in table III.

As λ is increased, a critical value λ_{cr} is reached at approximately $35.6°$ at which the position of the upper singular point coincides with that of the upper neutral point. If λ is increased beyond λ_{cr}, the procedures described above to determine the upper rear portion of the boundary no longer apply because it develops that θ_{N_U} is less than θ_{S_U} and the condition $\cos \psi \leq 0$ is violated on the portion of the boundary for which θ is between θ_{N_U} and θ_{S_U}. However, the integral curve from figure 6(b) that can be joined to the curve representing the forepart of the hollow at the point where $\cos \psi = 0$ satisfies the requirement that it extends downstream to infinity with $\cos \psi \leq 0$ everywhere. It follows that the front and upper rear curves can be joined smoothly at the point where $\theta = \theta_{N_U} = \theta_{S_U}$, that both portions of the boundary are parallel to the direction of the corpuscular stream at this point, and that the condition $\cos \psi \leq 0$ is satisfied at all points on the boundary. Since the values for ρ_{N_U} and θ_{N_U} are known from the solution for the front portion of the boundary, the appropriate values for K, designated K_U, for the upper rear portion of the boundary can be determined by direct substitution into equation (18) with lower signs. The resulting expression is

$$K_U = -\frac{3 \cos \theta_{S_F}}{\rho_{S_F}^2} + \frac{2 \cos \theta_{N_U}}{\rho_{N_U}^2} \qquad (33)$$

and the values for K_U for $\lambda = 35.6°$, $40°$, and $45°$ are 1.809, 1.789, and 1.770. The numerical values for the coordinates of the boundary for these values for λ are included in the lists given in tables II and III, and the results are presented graphically in figure 8.

SOLUTION FOR EQUATORIAL PLANE FOR $\lambda = 0$

The trace of the boundary of the hollow in the equatorial plane for the case $\lambda = 0$ can also be determined in a simple manner by numerical
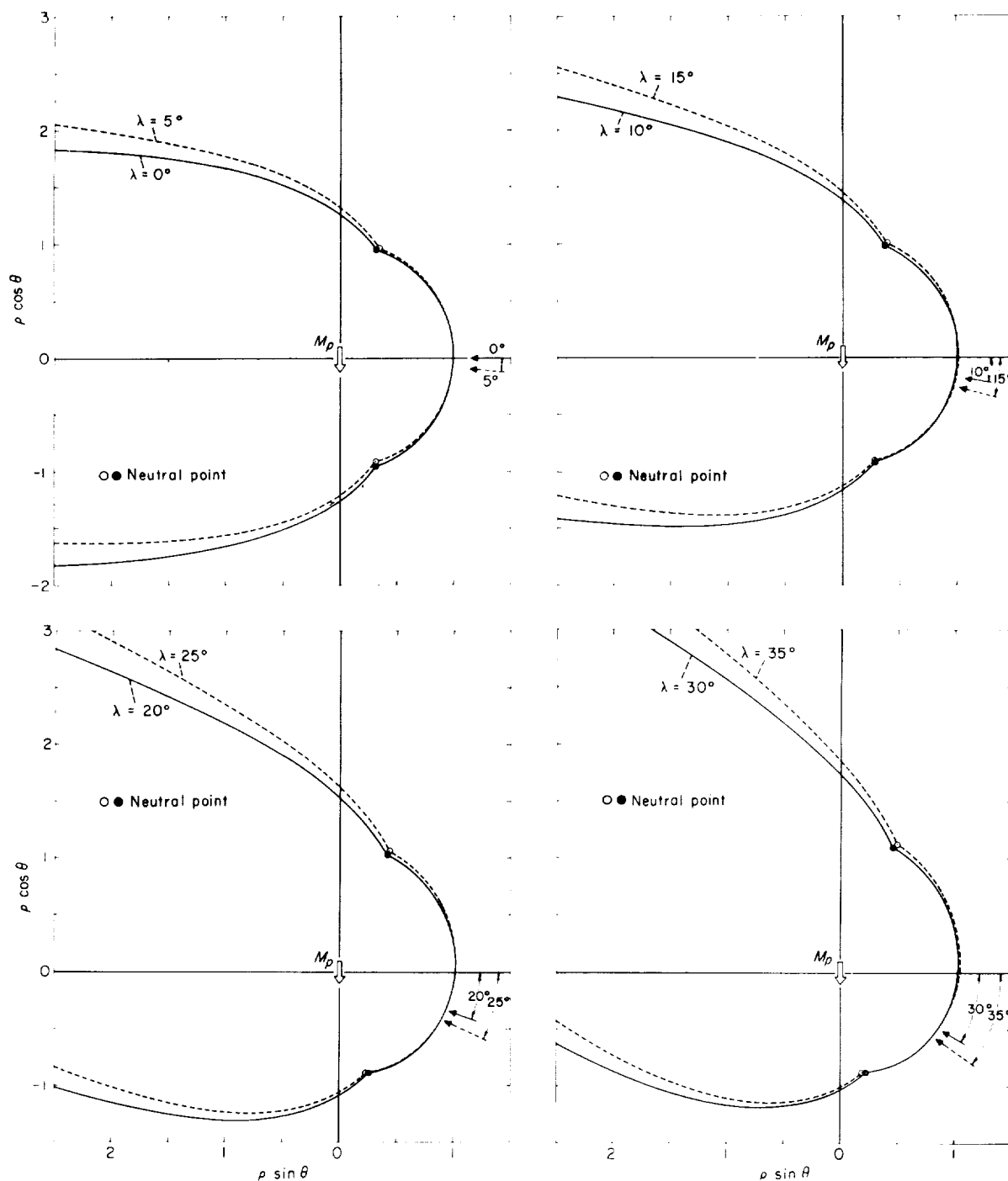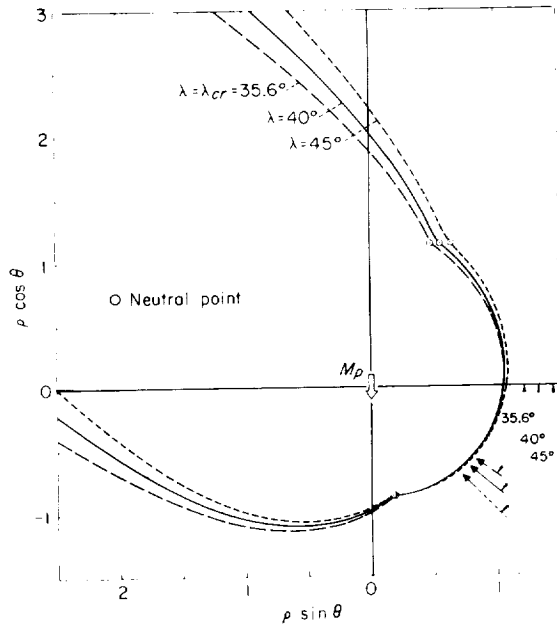

FIGURE 8.   Form of the boundary of the hollow in the meridian plane containing the dipole axis and the sun-earth line; $36.5° \leq \lambda \leq 45°$.

integration of the following differential equation obtained from equations (9), (12), and (13) by equating θ to $\pi/2$, λ, and $\partial\rho/\partial\theta$ to zero, and by restricting attention to the interval $\pi/2 \leq \varphi \leq 3\pi/2$:

$$\frac{d\rho}{d\varphi} = \rho \left(\frac{\rho^6 \sin \varphi \cos \varphi + \rho^6 - 1}{\rho^6 \cos^2 \varphi - 1} \right) \qquad (34)$$

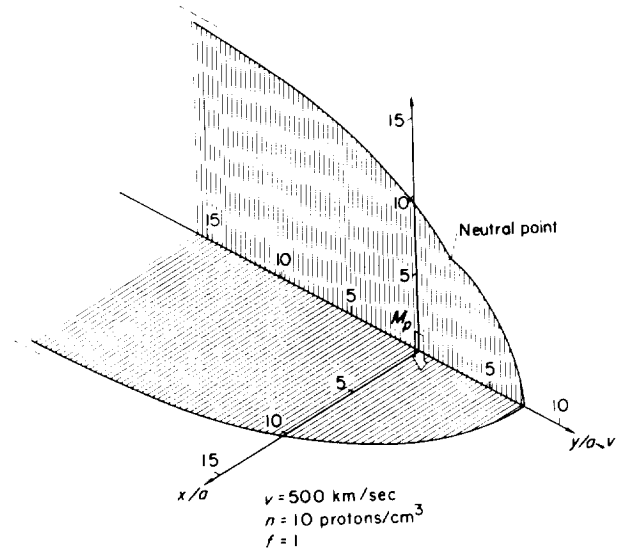$v = 500$ km/sec
$n = 10$ protons/cm³
$f = 1$

FIGURE 9.   Boundary of the hollow in the equatorial plane and the meridian plane containing the dipole axis and the sun-earth line; $\lambda = 0$.

A short table of values representing the solution has been given by Beard in reference 8. A more extensive table of values has been determined by the present authors and an abridged list of the results is given in table IV. The calculations were performed with an IBM 704 electronic computer using the fixed increment, fourth-order Adams-Moulton method together with the Runge-Kutta method to start the calculation at the apex of the hollow. The results were calculated using half-degree increments in φ, although only the results for 5° intervals are provided in table IV. These and the preceding results for the case in which $\lambda = 0$ are illustrated in graphical form in figure 9 for the representative conditions defined by values for r, n, and f of 500 km/sec, 10 protons/cm³, and 1.

TWO-DIMENSIONAL PROBLEM

DERIVATION OF APPROXIMATE DIFFERENTIAL EQUATION FOR THE COORDINATES OF THE BOUNDARY OF THE HOLLOW

Consider now the counterpart in two dimensions of the problem discussed in the preceding sections of this paper. Although it would be somewhat more natural to express the fundamental equations in a polar coordinate system, the spherical and Cartesian coordinate systems illustrated in figure 1 are retained to facilitate comparisons. Attention is thus confined to values for θ between 0 and π, and the notation $\sin(\pm\pi/2)$ is used to indicate the desired half plane in the same manner as in the three-dimensional problem. The fundamental relations are still given by equations (1) and (2) and the associated boundary conditions, but all quantities are required to be invariant with changes in x.

Equation (3) for the permanent magnetic field is thus replaced by equation (4), and the component thereof that lies in the surface of the hollow is given by

$$\hat{p} \cdot \mathbf{H}_{p_2} = -(b'M_{p_2}/r^2)\,[\sin\theta + (1/r)(dr/d\theta)\cos\theta] \quad (35)$$

Combination of this result with the fundamental approximate relations given by equations (1) and (8) and introduction of the dimensionless radius $\rho_2 = r/r_{0_2}$ where

$$r_{0_2} = \left(\frac{4f^2 M_{p_2}{}^2}{16\pi mn r^2}\right)^{1/4} = a\left(\frac{4f^2 H_{p_0}{}^2}{16\pi mn r^2}\right)^{1/4} \quad (36)$$

leads to the following differential equation for the shape of the surface of the hollow:

$$\pm \frac{1}{\rho_2{}^2}\left(\sin\theta + \frac{1}{\rho_2}\frac{d\rho_2}{d\theta}\cos\theta\right)$$

$$= \sin\theta\cos\lambda\sin\left(\pm\frac{\pi}{2}\right) - \cos\theta\sin\lambda$$

$$- \frac{1}{\rho_2}\frac{d\rho_2}{d\theta}\left[\cos\theta\cos\lambda\sin\left(\pm\frac{\pi}{2}\right) + \sin\theta\sin\lambda\right] \quad (37)$$

The significance of the alternative signs is the same as discussed following equations (13) and (14).

SOLUTION FOR TWO-DIMENSIONAL PROBLEM

As in the three-dimensional problem, it is convenient for the discussion of the solutions to drop the consistent use of plus and minus signs employed to this point and consider the two families of solutions associated with the following equation equivalent to equation (37):

$$\frac{d\rho_2}{d\theta} = -\rho_2\frac{\rho_2{}^2\sin|\theta - \lambda\sin(\pm\pi/2)| \mp \sin\theta}{\rho_2{}^2\cos|\theta - \lambda\sin(\pm\pi/2)| \pm \cos\theta} \quad (38)$$

The solutions are given by

$$\rho_2\cos\left[\theta - \lambda\sin\left(\pm\frac{\pi}{2}\right)\right] \mp \frac{1}{\rho_2}\cos\theta = K \quad (39)$$

where K is an arbitrary constant of integration, and the sign convention is the same as that described previously in connection with equations (17) and (18). The evaluation of K for the curves defining the boundary of the hollow requires consideration of the singular points in a manner analogous to that employed for the three-dimensional problem.

Results for $\lambda = 0$. The solutions given by equation (39) reduce for the case of $\lambda = 0$ to

$$\zeta_2 = \rho_2\cos\theta = \frac{K\rho_2{}^2}{\rho_2{}^2 \mp 1} \quad (40)$$

Plots of the integral curves are shown in figure 10 for several values for K. Examination of these curves reveals, for the same reasons as in the three-dimensional problem, that the desired solution is described by the unit circle

$$\rho_2 = 1 \quad (41)$$

(a) $\rho_2 \cos \theta = K \rho_2{}^2/(\rho_2{}^2 - 1)$

(b) $\rho_2 \cos \theta = K \rho_2{}^2/(\rho_2{}^2 + 1)$
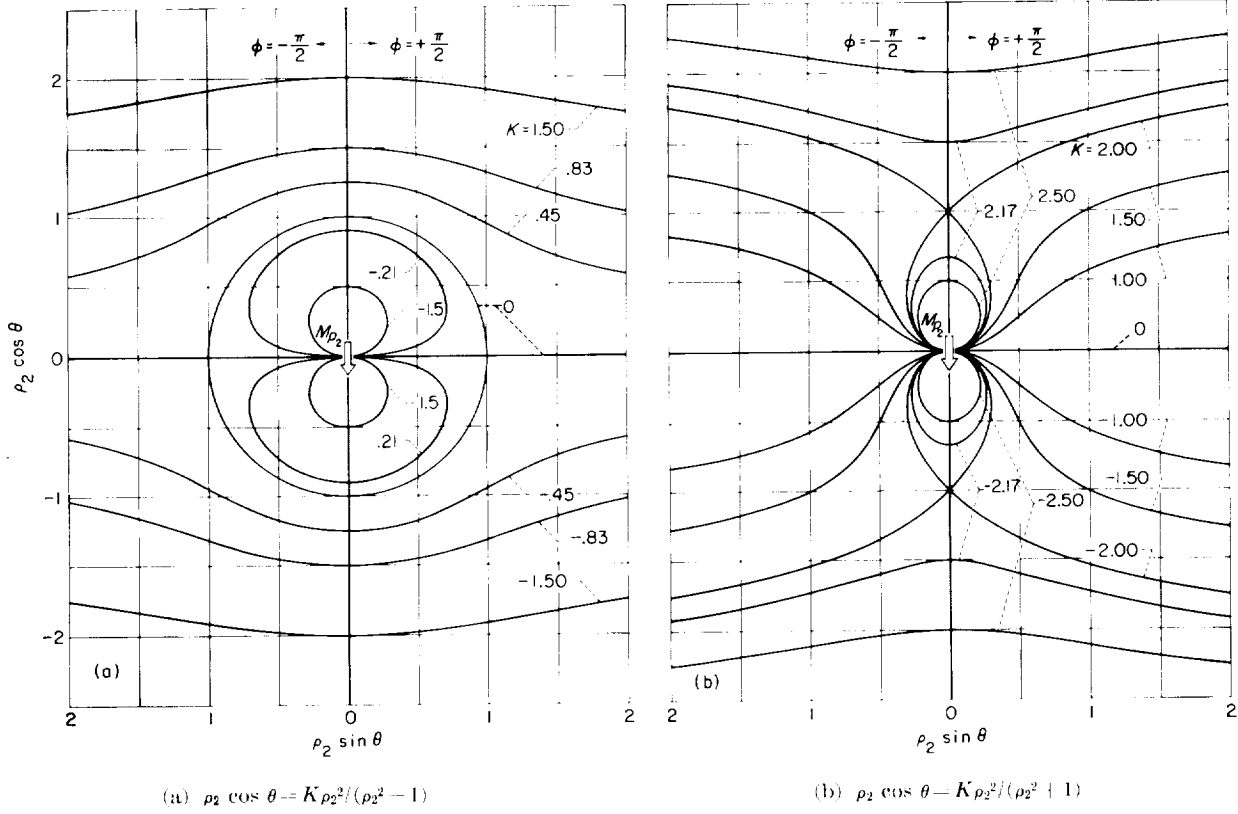
FIGURE 10. Integral curves defined by equation (40).
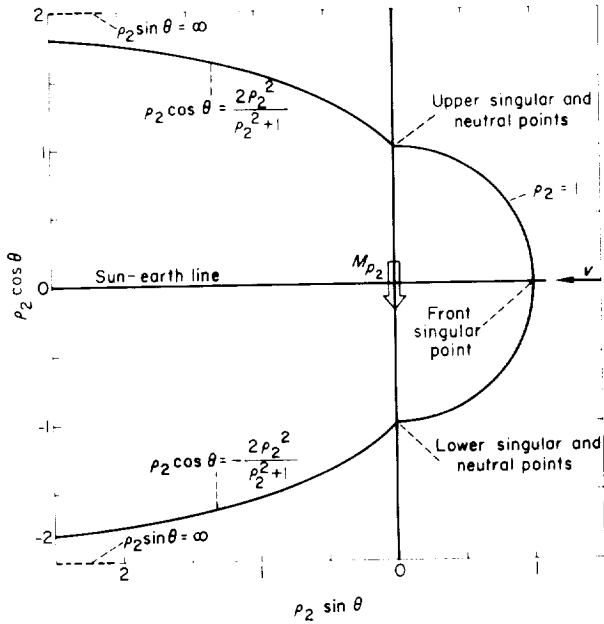
FIGURE 11.   Form of the boundary of the hollow in the two-dimensional problem; $\lambda = 0$.

for the region defined by $\varphi = \pi/2$, and by

$$\zeta_2 = \rho_2 \cos \theta = \pm \frac{2\rho_2{}^2}{\rho_2{}^2 + 1} \qquad (42)$$

for the region defined by $\varphi = -\pi/2$. The curves represented by equations (41) and (42) meet, of course, at the neutral points directly over the poles, and determine the form for the boundary of the hollow illustrated in figure 11. This result has been determined independently by Hurley (ref. 10).

Although the form of the hollow is generally similar in the two- and three-dimensional problems, it should be observed that the size of the hollow is much larger in the two-dimensional problem. Insertion into equation (36) of the same values that lead to a value for r_0/a of 7.6 in the three-dimensional problem leads to a value for r_{02}/a of 20.8 in the two-dimensional problem. The size of the hollow is also more sensitive to variations in the values selected for f in the two-dimensional problem. For example, arbitrary selec-

tion of 0.75 for f would reduce the values for r_0/a and r_{o2}/a by about 9 and 13 percent, respectively.

Results for arbitrary λ. The coordinates ρ_{2S} and θ_S of the singular points required for the evaluation of the integration constant K in equation (39) are determined by equating the numerator and denominator of the right-hand member of equation (38) to zero, and solving the two resulting algebraic equations simultaneously. This procedure leads to the following relations

$$\tan \theta_S + \tan [\theta_S - \lambda \sin (\pm \pi/2)] = 0 \qquad (43)$$

$$\rho_{2S} = 1 \qquad (44)$$

Equation (43) can be solved to yield explicit expressions for the angular coordinates of the singular points. Two singular points having coordinates given by

$$\theta_{S_F} = \frac{\pi}{2} + \frac{\lambda}{2}, \qquad \theta_{S_U} = \frac{\lambda}{2} \qquad (45)$$

are in the half plane defined by $\varphi = \pi/2$, and two having coordinates given by

$$\theta_{S_L} = \pi - \frac{\lambda}{2}, \qquad \theta_{S_R} = \frac{\pi}{2} - \frac{\lambda}{2} \qquad (46)$$

are in the half plane defined by $\varphi = -\pi/2$. The values for K associated with the integral curves that pass through the three singular points of interest in the following discussion are given in terms of the coordinates of the singular points by

$$K_{S_F} = -\frac{2 \cos \theta_{S_F}}{\rho_{2S_F}}, \qquad K_{S_U} = \frac{2 \cos \theta_{S_U}}{\rho_{2S_U}},$$

$$K_{S_L} = \frac{2 \cos \theta_{S_L}}{\rho_{2S_L}} \qquad (47)$$

or, more explicitly, by

$$K_{S_F} = 2 \sin \frac{\lambda}{2}, \qquad K_{S_U} = 2 \cos \frac{\lambda}{2},$$

$$K_{S_L} = -2 \cos \frac{\lambda}{2} \qquad (48)$$

The coordinates of the four singular points of equation (38) and of the two sets of integral curves defined by equation (39) are illustrated in figure 12 for the special case in which λ is 30°. The lines defined by $\theta = \theta_{S_U}$ and $\theta = \theta_{S_L}$ are also included on these plots, since considerations identical to those described in connection with equation (32) reveal that they are again the locus of points at which the integral curves are parallel to the direction of

the corpuscular stream. The curves of part (b) that pass through the upper and lower singular points remain exceptions, however.

Examination of the curves shown on figure 12 reveals, for the same reason as in the three-dimensional problem, that the desired solution for the front part of the boundary is provided by the integral curve from part (a) defined by $K = K_{S_F}$. The integral curves from part (b) defined by $K = K_{S_U}$ and $K = K_{S_L}$ pass through the upper and lower singular points and represent the counterpart of the curves selected to represent the upper and lower rear portions of the boundary for the three-dimensional case for λ less than $\lambda_{cr} = 35.6°$. Solution of the appropriate pairs of forms of equations (39) and (48) shows that the curves through the upper and lower singular points intersect the curve representing the front part of the boundary at the points

$$\theta = 0, \qquad \rho_2 = \frac{1}{\cos (\lambda/2) - \sin (\lambda/2)} \qquad (49)$$

and

$$\theta = \pi, \qquad \rho_2 = \frac{1}{\cos (\lambda/2) + \sin (\lambda/2)} \qquad (50)$$

Since the latter of these is on the sunward side of the lower singular point, the condition $\cos \psi \leq 0$ is satisfied and the integral curve through the lower singular point represents a portion of the boundary of the hollow. On the other hand, the upper intersection point indicated by equation (49) is farther from the sun than the upper singular point indicated by equation (45). It follows that the integral curve through the upper singular point can not be used to represent a portion of the boundary of the hollow, because the condition $\cos \psi \leq 0$ is violated along the front portion of the boundary for θ between 0 and $\lambda/2$. The desired solution can be obtained, however, by following the procedure described for the three-dimensional problem for λ greater than λ_{cr}, that is, by joining an integral curve from figure 12(b) to the integral curve representing the front part of the boundary at the point where $\theta = \theta_{S_U}$. The curves representing both the front and the upper rear portions of the boundary are parallel to the direction of the corpuscular stream at the point where they are joined and the condition $\cos \psi \leq 0$ is satisfied at all points on the boundary. The appropriate value for K that defines the curve for the upper

(a) $\rho_2 \cos\left[\theta - \lambda \sin\left(\cdot \frac{\pi}{2}\right)\right] - \frac{1}{\rho_2} \cos\theta = K$ (b) $\rho_2 \cos\left[\theta - \lambda \sin\left(\cdot \frac{\pi}{2}\right)\right] + \frac{1}{\rho_2} \cos\theta = K$
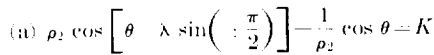
FIGURE 12.— Integral curves defined by equation (39), two-dimensional problem; $\lambda = 30°$.

rear portion of the boundary is designated K_r and can be determined by simple substitution. It is

$$K_r = 2 \qquad (51)$$

The form of the boundary of the hollow has been calculated using the procedure described above for several different values for λ ranging from 0° to 45°. The results are tabulated in tables V and VI, and an abridged series of plots showing the shape of the boundary for $\lambda = 0°$, 15°, 30°, and 45° is presented in figure 13. It should be observed that the scales employed to plot the results are proportional to $f^{1/2}\rho_2$ rather than ρ_2 alone so as to facilitate comparison in the next section with the results indicated by the exact solution in which the factor f does not appear. Results are shown for each λ for two different values for f, that is, for f equal unity, and for f equal to the particular value necessary for the

approximate solution to agree with the exact solution at the front singular point. The latter value is very nearly a constant independent of λ, varying only from 0.9125 to 0.9133 as λ varies from 0° to 45°. It can be seen from comparison with the results shown on figures 3, 7, and 8 that the shape of the hollow is generally similar in the two- and three-dimensional problems. As noted in the preceding section, however, differences between the normalizing distances r_0 and r_{0_2} defined by equations (12) and (36) are such that the size of the hollow associated with a given set of values for r, n, and H_{r_0} is much greater in the two-dimensional problem.

COMPARISON WITH EXACT SOLUTION

A measure of the accuracy of the approximate results presented in the preceding sections can be obtained by comparison with the corresponding results indicated by the exact solution of the two-
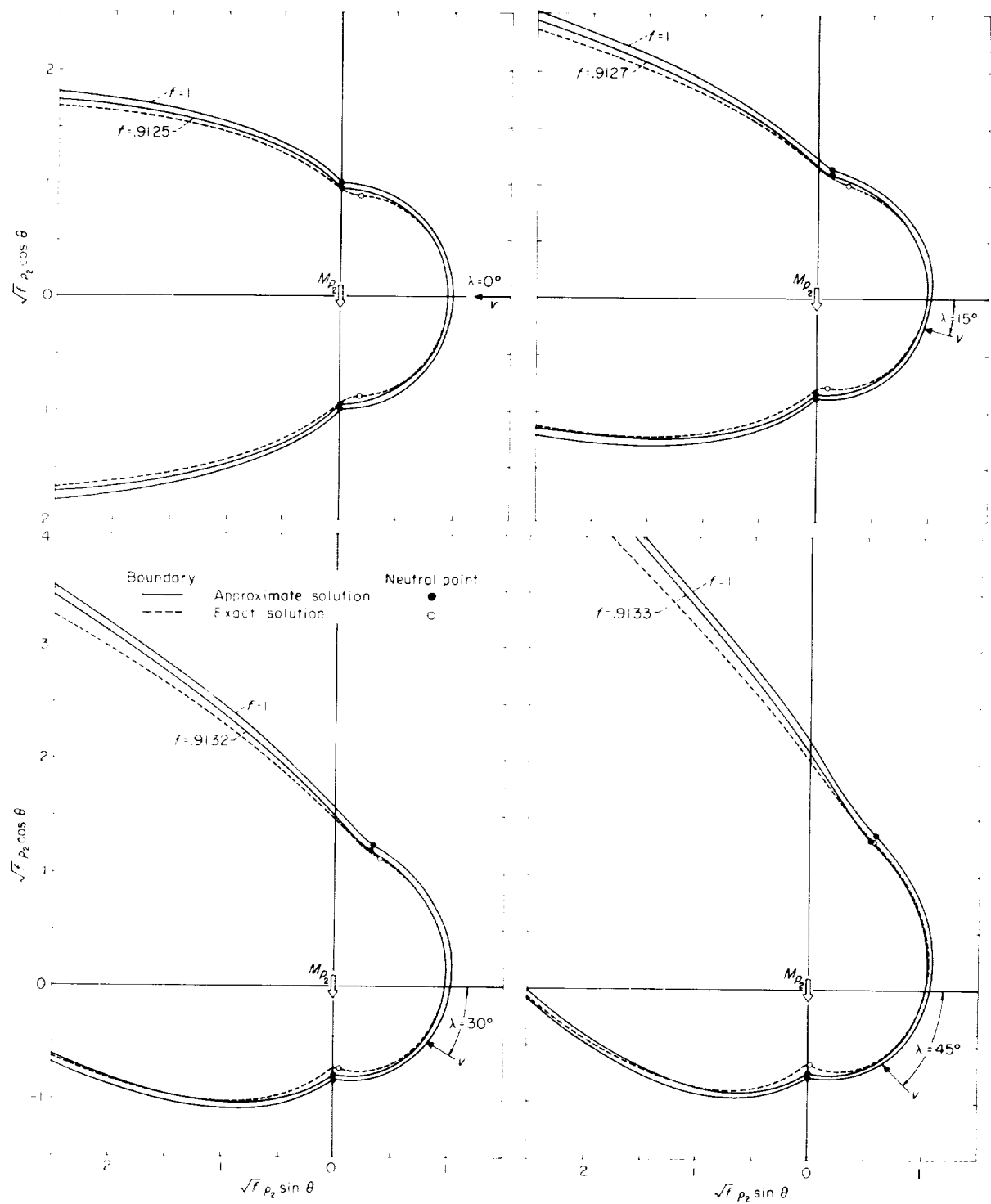
FIGURE 13.— Form of the boundary of the hollow, two-dimensional problem; $0° \leq \lambda \leq 45°$.

dimensional problem given by Zhigulev and Romishevskii (ref. 5), Hurley (ref. 10), and Dungey (ref. 6). The results indicated by the

exact solution are comparable with the approximate results given herein in that they are based on the same governing equations and boundary
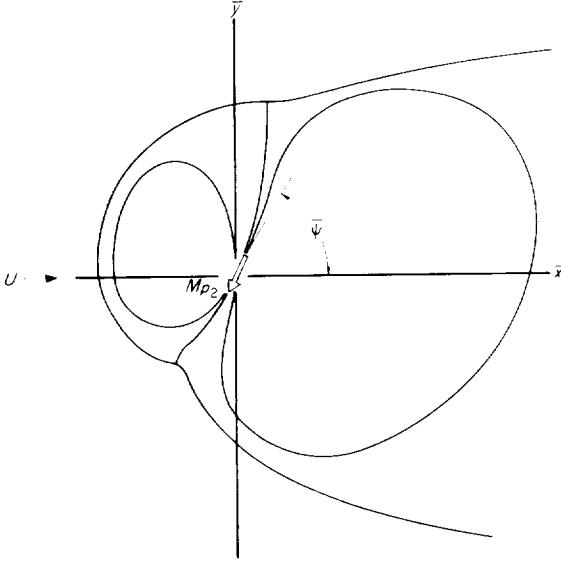
FIGURE 14. View of coordinate system and principal symbols used in exact solution by Zhigulev and Romishevskii (ref. 5).

conditions. They differ in that these equations are solved exactly rather than through the introduction of the approximation that H_s is equal to $2f$ times the tangential component of the permanent magnetic field.

The exact solution is obtained by application of conformal mapping techniques, and expressions are presented in parametric form for the coordinates of the boundary of the hollow. Dungey presents results for only the case $\lambda = 0$, but Zhigulev and Romishevskii and Hurley present results for arbitrary λ. The results are expressed in somewhat different forms in the three papers, but it can be shown that they are all equivalent for the cases to which they apply. The present calculations were performed using the formulation for the solution given by Zhigulev and Romishevskii, since it was desired to determine results for all λ, and Hurley's paper was not available at the time. The coordinate system employed by Zhigulev and Romishevskii is fixed with respect to the corpuscular stream rather than the earth, however, and the results for λ different from zero are of such form that they do not lend themselves to convenient conversion into the coordinate system employed herein. A sketch illustrating the coordinate system and principal symbols used in the latter paper is shown in figure 14.

The $\bar{x}$ coordinates of the boundary of the hollow are given by

$$\frac{\bar{x}(\bar{\varphi})}{A} = \frac{2}{\pi} \ln \frac{1}{2[1-\cos(\bar{\varphi}+\bar{\psi})]} + \frac{2}{\pi} \sum_{n=2}^{\infty} \frac{1+(-1)^n}{n(n^2-1)} \cos n\,\bar{\varphi}$$

(52)

where $\bar{\varphi}$ is a parameter that varies between 0 and 2π; A is a definite constant for any given $\bar{\psi}$, but its value is not given by Zhigulev and Romishevskii. If attention is restricted to positive values for $\bar{\psi}$, the $\bar{y}$ coordinates of the boundary are given by

$$\bar{y}/A = 1 + \cos \bar{\varphi} - 2\bar{\psi}/\pi \qquad \text{for} \quad 0 \leq \bar{\varphi} \leq \pi \qquad (53)$$

$$\bar{y}/A = -1 - \cos \bar{\varphi} - 2\bar{\psi}/\pi \quad \text{for} \quad \pi \leq \bar{\varphi} \leq 2\pi - \bar{\psi} \quad (54)$$

and

$$\bar{y}/A = 3 - \cos \bar{\varphi} - 2\bar{\psi}/\pi \qquad \text{for} \quad 2\pi - \bar{\psi} \leq \bar{\varphi} \leq 2\pi \quad (55)$$

Of the three expressions for $\bar{y}$, the first provides values corresponding to the front, the second to the lower rear, and the third to the upper rear portion of the boundary. The points at which the curves for the front and rear portions join are, of course, the neutral points. The corresponding values for $\bar{\varphi}$ are thus 0 or π. Of particular interest is the fact that the slope $d\bar{y}/d\bar{x}$ of the boundary is zero at the neutral points. This result, which can be ascertained readily from the ratio of the local values for $d\bar{y}/d\bar{\varphi}$ and $d\bar{x}/d\bar{\varphi}$, indicates that the boundary of the hollow is parallel to the direction of the corpuscular stream at the neutral points. It follows as a consequence of the fact that H_s, and hence also $\cos \psi$ according to equation (1), must vanish at a point where a magnetic line bifurcates.

The quantities $\bar{\psi}$, $\bar{x}$, and $\bar{y}$ that appear in equations (52) through (55) are related to λ, y, and z of the present analysis as follows:

$$\lambda = \frac{\pi}{2} - \bar{\psi} \tag{56}$$

$$y = -\bar{x} \cos \lambda + \bar{y} \sin \lambda \tag{57}$$

$$z = \bar{x} \sin \lambda + \bar{y} \cos \lambda \tag{58}$$

The coordinates of the boundary have been calculated using the above equations, and the results for the quantity $r/(1.078A)$ where $r^2 = \bar{x}^2 + \bar{y}^2$ are presented in tables VII and VIII. The factor 1.078 has been included so that $r/(1.078A)$ is unity to three decimal places at the position of the front singular point in the approximate two-dimensional analysis, that is, at the point where $\theta - \theta_{S_F} = (\pi + \lambda)/2$. The resulting values are thus directly comparable with the values for ρ_2 that are

obtained with the approximate analysis with the value for f selected so that the approximate and exact results agree at $\theta = \theta_{s_F}$. It should be noted that the factor required to reduce r/A to unity is not quite independent of λ, but varies between 1.0779 and 1.0784 as λ increases from $0°$ to $45°$.

The expression for A required to calculate the actual size of the hollow is not given by Zhigulev and Romishevskii, but can be determined from the solution given by Hurley in reference 10. It is, after adjusting for differences in nomenclature,

$$A = \sqrt{\frac{\pi}{2}} \frac{M_{\rho_2}}{(8\pi m n c^2)^{1/4}} = r_{0_2} \sqrt{\frac{\pi}{4f}} \approx \frac{0.886}{\sqrt{f}} r_{0_2} \quad (59)$$

These considerations lead to the concept of presenting comparisons of the results indicated by the exact and approximate solutions in terms of the quantity

$$f^{1/2} \rho_2 = 1.078 \sqrt{\frac{\pi}{4}} \left(\frac{r}{1.078A}\right) \approx 0.955 \left(\frac{r}{1.078A}\right) \quad (60)$$

rather than simply ρ_2. The necessary calculations have been performed, and the results are indicated by the dashed lines on figure 13 for comparison with the approximate results for the two-dimensional problem. It should be noted that the result indicated for $\lambda = 0$ differs somewhat from the corresponding result presented in figure 2 of reference 6 by Dungey since the latter contains a numerical error in the calculation of the x coordinate of the boundary.

It can be seen that the forms for the boundary of the hollow indicated by the approximate and exact solutions are in good agreement for all λ up to at least $45°$, with only minor differences occurring in the vicinity of the neutral points. The differences are slight in magnitude and local in extent, moreover, and it may be concluded that only a small loss of accuracy is incurred by introduction of the approximation that H_s is equal to $2f$ times the tangential component of the permanent magnetic field.

The size of the hollow indicated by the approximate theory depends upon the choice of value for f, however, and it can be seen that the procedure of simply equating f to unity leads to dimensions for the hollow that are about 5 percent too large. A substantial share of these differences is removed upon selection of a value of 0.913 for f for any λ between $0°$ and $45°$. This value, which can be

obtained readily from equation (60) by equating ρ^2 and $r/(1.078A)$ to unity and solving, may be contrasted with the value of 0.68 given by Ferraro in reference 9 for the case of a current carrying wire. The effects of this approximation have been evaluated only for the two-dimensional problem, but it is anticipated that the results would be of comparable quality for the three-dimensional case. It is possible, since f enters as the cube root in the three-dimensional case compared with the square root in the two-dimensional case, that the accuracy of the approximate results may even be somewhat better in the three-dimensional problem.

CONCLUDING REMARKS

The results of a theoretical investigation of the form of the hollow carved out of a neutral stream of ionized solar corpuscles by interaction with a magnetic dipole representing the geomagnetic field have been presented in the preceding paragraphs. The basic concepts of the analysis are classical and stem from a long series of investigations of Chapman, Ferraro, Dungey, and others. The equations have been simplified by the introduction of a single assumption suggested and commented upon recently by Beard and Ferraro in references 8 and 9. Analytic and numerical solutions have been determined without recourse to further approximations. The results are consistent with those indicated by earlier theoretical studies, but this is as should be expected, since the latter are based on essentially the same concepts as the present calculations. The corresponding problem in two dimensions is also considered, and it is shown that the analogous approximate results are in good agreement with the results indicated by the exact solution given recently by Zhigulev and Romishevskii (ref. 5), Hurley (ref. 10), and Dungey (ref. 6). Although a similar check on the accuracy of the approximate results for the three-dimensional case can not be accomplished at the present time, it is anticipated that the results given herein represent good approximations to the exact solutions.

The size of the hollow indicated by the theoretical studies is nevertheless not in good agreement with that indicated by magnetometer data from Pioneer V reported recently by Coleman, Sonett, Judge, and Smith in reference 15. These data, acquired in the vicinity of the equatorial plane

on the afternoon side of the earth, show that the geomagnetic field terminates at a distance of about 14 earth radii from the center of the earth. This result may be compared with the distance of about 7 to 10 earth radii indicated by the present calculations when representative values are used for the velocity r and number density n of the corpuscular stream. This is a large discrepancy which can not be resolved by simply choosing different values for r and n since the necessary values are unacceptably small.

The magnetometer data from Pioneer V, and also from Explorer VI, display variations that have been interpreted by Smith, Coleman, Judge, and Sonett in reference 16 as indicating the presence of a westward flowing current of about 5×10^6 amperes distributed over a large volume having the form of a toroidal ring situated in the magnetic equatorial plane at a distance of about 10 earth radii. The magnetic moment of such a current system is of the same sign and order of magnitude as that of the main dipole field. It is apparent that the presence of the ring current has the effect of greatly increasing the size, as well as altering the form, of the hollow. The present investigation has been extended, therefore, to determine the effects of an equatorial ring current: It has been found, for the case in which $r = 500$ km/sec, $n = 10$ protons/cm^3, $\lambda = 0°$, and $f = 1$, that the geocentric distance to the intersection of the boundary of the hollow and the sun-earth line, which is about 7.6 earth radii for the dipole alone, increases to about 12.0 earth radii with the addition of a ring current of 5×10^6 amperes having infinitesimal cross section and situated in the magnetic equatorial plane at a distance of 10 earth radii. While this model is admittedly highly simplified, the calculated distance to the boundary of the hollow is compatible with the observed distance. It thus appears that the addition of the magnetic field of a ring current will suffice to remove the major part of the discrepancy noted above.

AMES RESEARCH CENTER
NATIONAL AERONAUTICS AND SPACE ADMINISTRATION
MOFFET FIELD, CALIF., JUNE 9, 1961

REFERENCES

1. Chapman, Sydney: Idealized Problems of Plasma Dynamics Relating to Geomagnetic Storms. Reviews of Modern Physics, vol. 32, no. 4, Oct. 1960, pp. 919–933.

2. Ferraro, V. C. A.: Theory of Sudden Commencements and of the First Phase of a Magnetic Storm. Reviews of Modern Physics, vol. 32, no. 4, Oct. 1960, pp. 934–940.

3. Parker, E. N.: The Hydrodynamic Treatment of the Expanding Solar Corona. Astrophysical Journal, vol. 132, no. 1, July 1960, pp. 175–183.

4. Parker, E. N.: The Hydrodynamic Theory of Solar Corpuscular Radiation and Stellar Winds. Astrophysical Journal, vol. 132, no. 3, Nov. 1960, pp. 821–866.

5. Zhigulev, V. N., and Romishevskii, E. A.: Concerning the Interaction of Currents Flowing in a Conducting Medium with the Earth's Magnetic Field. Doklady Akad. Nauk SSSR, vol. 127, no. 5, 1959, pp. 1001–1004. (English translation: Soviet Physics Doklady, vol. 4, no. 4, Feb. 1960, pp. 859–862.)

6. Dungey, J. W.: The Steady State of the Chapman-Ferraro Problem in Two Dimensions. Jour. Geophys. Research, vol. 66, no. 4, April 1961, pp. 1043–1047.

7. Obayashi, Tatsuzo, and Hakura, Yukio: Enhanced Ionization in the Polar Ionosphere Associated With Geomagnetic Storms. Jour. Atmospheric and Terrestrial Physics, vol. 18, no. 213, June 1960, pp. 101–122.

8. Beard, David B.: The Interaction of the Terrestrial Magnetic Field With the Solar Corpuscular Radiation. Jour. Geophys. Research, vol. 65, no. 11, Nov. 1960, pp. 3559–3568.

9. Ferraro, V. C. A.: An Approximate Method of Estimating the Size and Shape of the Stationary Hollow Carved Out in a Neutral Ionized Stream of Corpuscles Impinging on the Geomagnetic Field. Jour. Geophys. Research, vol. 65, no. 12, Dec. 1960, pp. 3951–3953.

10. Hurley, James: Interaction Between the Solar Wind and the Geomagnetic Field. New York University Report, March 1961.

11. Ferraro, V. C. A.: On the Theory of the First Phase of a Geomagnetic Storm: A New Illustrative Calculation Based on an Idealized (Plane not Cylindrical) Model Field Distribution. Jour. Geophys. Research, vol. 57, no. 1, March 1952, pp. 15–49.

12. Dungey, J. W.: Cosmic Electrodynamics. Cambridge, University Press, 1958.

13. Piddington, J. H.: Geomagnetic Storm Theory. Jour. Geophys. Research, vol. 65, no. 1, Jan. 1960, pp. 93–106.

14. Spreiter, John R., and Briggs, Benjamin R.: Theoretical Determination of the Boundary of the Solar Corpuscular Stream Produced by Interaction with the Magnetic Dipole Field of the Earth. Jour. Geophys. Research, vol. 67, no. 1, Jan. 1962, pp. 37–51.

15. Coleman, P. J., Jr., Sonett, C. P., Judge, D. L., and Smith, E. J.: Some Preliminary Results of the Pioneer V Magnetometer Experiment. Jour. Geophys. Research, vol. 65, no. 6, June 1960, pp. 1856–1857.

16. Smith, E. J., Coleman, P. J., Judge, D. L., and Sonett, C. P.: Characteristics of the Extraterrestrial Current System: Explorer VI and Pioneer V. Jour. Geophys. Research, vol. 65, no. 6, June 1960, pp. 1858–1861.

TABLE I.—VALUES FOR θ_S, ρ_S, AND K_S FOR VARIOUS λ

λ, deg	θ_{S_F}, deg	ρ_{S_F}	K_{S_F}	θ_{S_U}, deg	ρ_{S_U}	K_{S_U}	θ_{S_L}, deg	ρ_{S_L}	K_{S_L}
0	90.00	1.0000	0	0	1.2600	1.8900	180.00	1.2600	−1.8900
5	91.67	1.0004	.0872	3.33	1.2594	1.8884	176.67	1.2594	−1.8884
10	93.34	1.0017	.1742	6.66	1.2578	1.8836	173.34	1.2578	−1.8836
15	95.03	1.0038	.2608	9.97	1.2551	1.8756	170.03	1.2551	1.8756
20	96.73	1.0067	.3467	13.27	1.2515	1.8644	−166.73	1.2515	1.8644
25	98.45	1.0105	.4317	16.55	1.2468	1.8500	−163.45	1.2468	1.8500
30	100.20	1.0151	.5157	19.80	1.2411	1.8324	−160.20	1.2411	−1.8324
35	101.99	1.0205	.5984	23.01	1.2346	1.8116	−156.99	1.2346	1.8116
35.6	102.21	1.0212	.6082	23.39	1.2337	1.8089	−156.61	1.2337	1.8089
40	103.81	1.0267	.6796	26.19	1.2272	1.7876	−153.81	1.2272	−1.7876
45	105.68	1.0336	.7591	29.32	1.2190	1.7605	150.68	1.2190	−1.7605

TABLE II.—COORDINATES θ AND ρ OF BOUNDARY OF HOLLOW IN THE MERIDIAN PLANE CONTAINING THE DIPOLE AXIS AND THE SUN-EARTH LINE FOR VARIOUS λ

$$\varphi - \frac{\pi}{2}$$

θ, deg	λ, deg										
	0	5	10	15	20	25	30	35	35.6	40	45
0	1.260	1.316	1.378	1.448	1.529	1.622	1.730	1.858	1.875	2.013	2.215
5	1.186	1.286	1.288	1.347	1.414	1.493	1.583	1.688	1.702	1.815	1.978
10	1.116	1.157	1.202	1.246	1.314	1.380	1.455	1.542	1.553	1.646	1.782
15	1.051	1.086	1.126	1.170	1.276	1.278	1.341	1.413	1.423	1.501	1.618
20	1.000	1.022	1.054	1.093	1.135	1.183	1.231	1.299	1.307	1.375	1.479
25	1.000	1.020	1.043	1.069	1.100	1.135	1.176	1.223	1.229	1.274	1.369
30	1.000	1.018	1.039	1.063	1.091	1.123	1.160	1.202	1.208	1.252	1.310
35	1.000	1.016	1.035	1.057	1.083	1.112	1.145	1.183	1.188	1.228	1.279
40	1.000	1.015	1.032	1.052	1.075	1.101	1.131	1.166	1.171	1.206	1.252
45	1.000	1.013	1.029	1.047	1.067	1.091	1.119	1.150	1.154	1.186	1.228
50	1.000	1.012	1.025	1.042	1.060	1.082	1.107	1.136	1.139	1.168	1.206
55	1.000	1.010	1.022	1.037	1.054	1.073	1.096	1.122	1.125	1.151	1.185
60	1.000	1.009	1.019	1.032	1.047	1.065	1.085	1.109	1.112	1.136	1.166
65	1.000	1.007	1.017	1.028	1.041	1.057	1.076	1.097	1.099	1.121	1.149
70	1.000	1.006	1.014	1.024	1.036	1.050	1.066	1.085	1.088	1.107	1.132
75	1.000	1.005	1.011	1.020	1.030	1.042	1.057	1.074	1.076	1.094	1.116
80	1.000	1.003	1.009	1.016	1.024	1.035	1.048	1.063	1.065	1.081	1.101
85	1.000	1.002	1.006	1.012	1.019	1.028	1.040	1.053	1.055	1.069	1.087
90	1.000	1.001	1.003	1.008	1.014	1.021	1.031	1.043	1.045	1.057	1.074
95	1.000	1.000	1.001	1.004	1.008	1.015	1.023	1.034	1.035	1.046	1.060
100	1.000	.998	.998	1.000	1.003	1.009	1.015	1.024	1.025	1.035	1.048
105	1.000	.997	.996	.996	.998	1.002	1.008	1.015	1.016	1.024	1.035
110	1.000	.996	.993	.992	.993	.996	1.000	1.006	1.007	1.014	1.023
115	1.000	.995	.991	.989	.988	.989	.992	.997	.998	1.003	1.011
120	1.000	.993	.988	.985	.983	.983	.985	.988	.989	.993	1.000
125	1.000	.992	.985	.981	.978	.977	.977	.979	.979	.983	.988
130	1.000	.990	.983	.977	.973	.970	.969	.970	.970	.973	.977
135	1.000	.989	.980	.973	.967	.964	.962	.961	.961	.962	.965
140	1.000	.988	.977	.969	.962	.957	.954	.952	.952	.952	.954
145	1.000	.986	.974	.964	.957	.950	.946	.943	.943	.942	.942
150	1.000	.984	.971	.960	.951	.944	.938	.934	.934	.932	.931
155	1.000	.983	.968	.956	.945	.936	.930	.924	.924	.921	.919
160	1.000	.981	.965	.951	.939	.929	.921	.915	.914	.910	.907
165	1.000	1.018	.989	.963	.939	.922	.912	.905	.904	.899	.895
170	1.051	1.079	1.045	1.015	.988	.964	.941	.921	.919	.903	.887
175	1.186	1.142	1.104	1.070	1.039	1.011	.986	.963	.961	.943	.924
180	1.260	1.210	1.167	1.128	1.093	1.061	1.032	1.007	1.004	.983	.962

TABLE II. COORDINATES θ AND ρ OF BOUNDARY OF HOLLOW IN THE MERIDIAN PLANE CONTAINING THE DIPOLE AXIS AND THE SUN-EARTH LINE FOR VARIOUS λ Concluded

$$\varphi = -\frac{\pi}{2}$$

θ, deg	λ, deg										
	0	5	10	15	20	25	30	35	35.6	40	45
0	1.260	1.316	1.378	1.448	1.529	1.622	1.730	1.858	1.875	2.013	2.215
5	1.341	1.405	1.478	1.561	1.657	1.768	1.900	2.058	2.079	2.252	2.507
10	1.430	1.505	1.590	1.688	1.803	1.939	2.101	2.298	2.325	2.547	2.879
15	1.528	1.616	1.717	1.834	1.973	2.140	2.342	2.595	2.630	2.922	3.370
20	1.639	1.742	1.862	2.004	2.174	2.382	2.641	2.973	3.019	3.417	4.053
25	1.764	1.886	2.031	2.205	2.417	2.682	3.022	3.473	3.537	4.106	5.072
30	1.907	2.055	2.232	2.448	2.718	3.065	3.525	4.169	4.263	5.135	6.766
35	2.075	2.255	2.475	2.749	3.102	3.572	4.227	5.208	5.360	6.845	
40	2.273	2.497	2.776	3.134	3.611	4.278	5.277	6.938	7.215		
45	2.514	2.797	3.161	3.645	4.322	5.336	7.024				
50	2.814	3.182	3.672	4.358	5.386	7.099					
55	3.197	3.693	4.386	5.427	7.160						
60	3.707	4.407	5.458	7.210							6.843
65	4.420	5.480	7.247						9.857	6.941	5.193
70	5.492	7.271						7.026	6.754	5.263	4.211
75	7.283						7.100	5.375	5.169	4.263	3.562
80						7.161	5.418	4.347	4.209	3.602	3.101
85					7.210	5.418	4.347	3.636	3.567	3.132	2.757
90				7.247	5.451	4.377	3.665	3.158	3.107	2.781	2.490
95			7.271	5.475	4.401	3.687	3.180	2.801	2.762	2.508	2.276
100		7.284	5.490	4.417	3.703	3.196	2.817	2.523	2.493	2.290	2.101
105	7.283	5.496	4.426	3.714	3.207	2.828	2.534	2.301	2.276	2.111	1.955
110	5.492	4.427	3.718	3.212	2.834	2.541	2.308	2.119	2.098	1.961	1.830
115	4.420	3.716	3.213	2.836	2.544	2.312	2.122	1.966	1.949	1.834	1.722
120	3.707	3.208	2.833	2.543	2.312	2.123	1.967	1.835	1.821	1.723	1.627
125	3.197	2.826	2.538	2.308	2.120	1.965	1.834	1.722	1.710	1.626	1.543
130	2.814	2.528	2.300	2.114	1.960	1.829	1.718	1.623	1.612	1.540	1.468
135	2.514	2.289	2.105	1.951	1.822	1.712	1.617	1.535	1.526	1.463	1.399
140	2.273	2.092	1.940	1.812	1.703	1.609	1.527	1.456	1.448	1.393	1.337
145	2.075	1.925	1.799	1.691	1.598	1.517	1.446	1.384	1.377	1.329	1.280
150	1.907	1.783	1.677	1.585	1.505	1.435	1.373	1.318	1.312	1.270	1.230
155	1.764	1.659	1.569	1.490	1.421	1.360	1.306	1.258	1.253	1.214	1.175
160	1.639	1.550	1.473	1.405	1.345	1.292	1.249	1.201	1.196	1.163	1.129
165	1.528	1.453	1.386	1.327	1.276	1.226	1.185	1.148	1.144	1.115	1.084
170	1.430	1.365	1.308	1.265	1.209	1.168	1.132	1.099	1.095	1.069	1.042
175	1.341	1.286	1.233	1.189	1.149	1.113	1.081	1.052	1.048	1.025	1.001
180	1.260	1.210	1.167	1.128	1.093	1.061	1.032	1.007	1.004	.983	.962

TABLE III. COORDINATES θ_N AND ρ_N OF NEUTRAL POINTS FOR VARIOUS λ

	λ, deg										
	0	5	10	15	20	25	30	35	35.6	40	45
θ_{N_U}, deg	19.10	19.50	20.75	21.00	22.20	22.40	22.50	23.60	23.39	26.19	29.32
ρ_{N_U}	1.000	1.023	1.043	1.053	1.103	1.142	1.183	1.235	1.239	1.275	1.303
θ_{N_L}, deg	161.00	161.0	163.0	163.4	163.75	165.4	165.7	167.5	167.7	168.50	169.2
ρ_{N_L}	1.000	.960	.960	.942	.923	.920	.900	.890	.890	0.886	.880

TABLE IV.—COORDINATES OF BOUNDARY OF HOLLOW IN THE EQUATORIAL PLANE, $\lambda = 0$

φ, deg	ρ	φ, deg	ρ
90.00	1.0000	180.00	1.3491
95.00	1.0008	185.00	1.4053
100.00	1.0032	190.00	1.4698
105.00	1.0072	195.00	1.5444
110.00	1.0129	200.00	1.6310
115.00	1.0203	205.00	1.7326
120.00	1.0295	210.00	1.8528
125.00	1.0406	215.00	1.9969
130.00	1.0537	220.00	2.1719
135.00	1.0689	225.00	2.3881
140.00	1.0865	230.00	2.6612
145.00	1.1066	235.00	3.0156
150.00	1.1296	240.00	3.4919
155.00	1.1557	245.00	4.1635
160.00	1.1852	250.00	5.1767
165.00	1.2187	255.00	6.8735
170.00	1.2567	260.00	10.2794
175.00	1.2999		

TABLE V.—COORDINATES θ AND ρ_2 OF BOUNDARY FOR VARIOUS λ, TWO-DIMENSIONAL PROBLEM

$$\varphi = \frac{\pi}{2}$$

θ, deg	λ, deg									
	0	5	10	15	20	25	30	35	40	45
0	1.000	1.066	1.141	1.226	1.326	1.441	1.577	1.740	1.937	2.180
5	1.000	1.043	1.091	1.155	1.236	1.333	1.447	1.583	1.744	1.941
10	1.000	1.039	1.083	1.134	1.192	1.264	1.355	1.465	1.598	1.758
15	1.000	1.036	1.076	1.122	1.174	1.234	1.303	1.388	1.493	1.622
20	1.000	1.033	1.069	1.111	1.159	1.213	1.274	1.346	1.428	1.528
25	1.000	1.030	1.063	1.101	1.144	1.193	1.248	1.312	1.385	1.470
30	1.000	1.027	1.057	1.092	1.131	1.175	1.225	1.282	1.347	1.423
35	1.000	1.024	1.052	1.083	1.118	1.158	1.203	1.254	1.313	1.380
40	1.000	1.022	1.047	1.075	1.106	1.141	1.183	1.229	1.282	1.342
45	1.000	1.019	1.042	1.067	1.095	1.128	1.165	1.206	1.253	1.307
50	1.000	1.017	1.037	1.059	1.085	1.114	1.147	1.185	1.227	1.275
55	1.000	1.015	1.032	1.052	1.075	1.101	1.131	1.164	1.202	1.245
60	1.000	1.013	1.028	1.046	1.066	1.089	1.115	1.145	1.179	1.218
65	1.000	1.011	1.024	1.039	1.057	1.077	1.101	1.127	1.158	1.192
70	1.000	1.009	1.020	1.033	1.048	1.066	1.087	1.110	1.137	1.168
75	1.000	1.007	1.016	1.026	1.040	1.055	1.073	1.094	1.118	1.145
80	1.000	1.005	1.012	1.020	1.031	1.045	1.061	1.078	1.099	1.123
85	1.000	1.003	1.008	1.015	1.023	1.034	1.048	1.063	1.081	1.102
90	1.000	1.001	1.004	1.009	1.015	1.024	1.035	1.049	1.064	1.082
95	1.000	.999	1.000	1.003	1.008	1.015	1.023	1.034	1.048	1.063
100	1.000	.997	.997	.997	1.000	1.005	1.012	1.020	1.031	1.045
105	1.000	.995	.992	.993	.992	.995	1.000	1.007	1.016	1.026
110	1.000	.993	.989	.986	.987	.986	.989	.993	1.000	1.009
115	1.000	.991	.985	.980	.977	.977	.977	.980	.985	.991
120	1.000	.989	.981	.974	.970	.967	.967	.967	.970	.974
125	1.000	.987	.977	.968	.962	.957	.955	.954	.955	.957
130	1.000	.985	.973	.963	.954	.948	.943	.941	.941	.941
135	1.000	.983	.969	.957	.946	.938	.932	.927	.925	.921
140	1.000	.981	.965	.950	.938	.928	.920	.914	.910	.907
145	1.000	.979	.960	.944	.930	.918	.909	.901	.895	.890
150	1.000	.976	.956	.937	.922	.908	.897	.887	.879	.874
155	1.000	.974	.951	.931	.913	.898	.884	.873	.864	.856
160	1.000	.971	.946	.924	.904	.887	.872	.859	.848	.839
165	1.000	.969	.941	.916	.894	.875	.859	.844	.832	.821
170	1.000	.966	.935	.908	.885	.864	.845	.829	.815	.803
175	1.000	.962	.929	.900	.874	.851	.831	.814	.798	.785
180	1.000	.959	.923	.891	.863	.838	.817	.797	.780	.765

TABLE V. COORDINATES θ AND ρ_2 OF BOUNDARY FOR VARIOUS λ, TWO-DIMENSIONAL PROBLEM Concluded

$$\varphi = \frac{\pi}{2}$$

θ, deg	λ, deg									
	0	5	10	15	20	25	30	35	40	45
0	1.000	1.066	1.141	1.226	1.326	1.441	1.577	1.740	1.937	2.180
5	1.091	1.155	1.236	1.333	1.447	1.583	1.744	1.941	2.183	2.489
10	1.192	1.264	1.355	1.465	1.598	1.758	1.952	2.194	2.498	2.894
15	1.303	1.388	1.493	1.622	1.779	1.971	2.210	2.514	2.908	3.438
20	1.428	1.528	1.653	1.807	1.996	2.233	2.535	2.927	3.456	4.203
25	1.570	1.690	1.840	2.027	2.262	2.561	2.952	3.479	4.225	5.353
30	1.732	1.879	2.063	2.295	2.592	2.980	3.506	4.250	5.377	7.267
35	1.921	2.102	2.332	2.626	3.013	3.537	4.280	5.404	7.293	
40	2.144	2.372	2.664	3.049	3.571	4.312	5.436	7.323		
45	2.414	2.705	3.088	3.608	4.348	5.470	7.356			
50	2.748	3.129	3.648	4.386	5.506	7.391				
55	3.172	3.689	4.426	5.545	7.429					
60	3.732	4.468	5.586	7.469						7.400
65	4.511	5.628	7.510						7.480	5.622
70	5.671	7.552						7.545	5.671	4.550
75	7.596						7.596	5.710	4.581	3.831
80						7.632	5.737	4.603	3.849	3.313
85					7.654	5.753	4.616	3.860	3.322	2.921
90				7.661	5.759	4.620	3.864	3.326	2.924	2.613
95			7.654	5.753	4.616	3.860	3.322	2.921	2.611	2.364
100		7.632	5.737	4.603	3.849	3.313	2.913	2.603	2.357	2.157
105	7.596	5.710	4.581	3.831	3.297	2.899	2.591	2.346	2.147	1.983
110	5.671	4.550	3.805	3.275	2.879	2.573	2.330	2.133	1.970	1.833
115	4.511	3.772	3.247	2.855	2.551	2.310	2.114	1.953	1.817	1.702
120	3.732	3.212	2.824	2.524	2.286	2.092	1.932	1.798	1.684	1.587
125	3.172	2.789	2.492	2.257	2.065	1.907	1.775	1.663	1.567	1.484
130	2.748	2.456	2.224	2.035	1.879	1.749	1.638	1.544	1.462	1.391
135	2.414	2.186	2.001	1.848	1.720	1.611	1.518	1.437	1.368	1.307
140	2.144	1.963	1.813	1.687	1.580	1.489	1.410	1.342	1.282	1.229
145	1.921	1.774	1.651	1.547	1.457	1.380	1.313	1.254	1.203	1.158
150	1.732	1.612	1.510	1.423	1.347	1.282	1.225	1.175	1.131	1.092
155	1.570	1.470	1.385	1.312	1.248	1.193	1.144	1.101	1.063	1.030
160	1.428	1.346	1.274	1.213	1.159	1.111	1.069	1.033	1.000	0.971
165	1.303	1.234	1.174	1.122	1.076	1.036	1.000	0.969	0.941	0.916
170	1.192	1.134	1.083	1.039	1.000	0.966	0.935	0.908	0.885	0.864
175	1.091	1.043	1.000	0.962	0.929	0.900	0.874	0.851	0.831	0.814
180	1.000	0.959	0.923	0.891	0.863	0.838	0.817	0.797	0.780	0.765

TABLE VI. COORDINATES θ_N AND ρ_{2N} OF NEUTRAL POINTS FOR VARIOUS λ, TWO-DIMENSIONAL PROBLEM

	λ, deg									
	0	5	10	15	20	25	30	35	40	45
θ_{N_U}, deg	0	2.5	5.0	7.5	10.0	12.5	15.0	17.5	20.0	22.5
ρ_{2N_U}	1.000	1.044	1.091	1.140	1.192	1.246	1.303	1.364	1.428	1.497
θ_{N_L}, deg	180.0	180.0	180.0	180.0	180.0	180.0	180.0	180.0	180.0	180.0
ρ_{2N_L}	1.000	0.959	0.923	0.891	0.863	0.838	0.817	0.797	0.780	0.765

TABLE VII. COORDINATES θ AND r/(1.078A) OF THE BOUNDARY OF THE HOLLOW FOR VARIOUS λ. EXACT SOLUTION FOR TWO-DIMENSIONAL PROBLEM

$$\varphi = \frac{\pi}{2}$$

θ, deg	λ, deg									
	0	5	10	15	20	25	30	35	40	45
0	0.993	1.056	1.127	1.210	1.304	1.415	1.545	1.699	1.885	2.113
5	.950	1.004	1.067	1.138	1.221	1.316	1.428	1.559	1.716	1.904
10	.943	.986	1.036	1.096	1.166	1.247	1.342	1.454	1.586	1.744
15	.956	.992	1.034	1.082	1.139	1.206	1.286	1.380	1.491	1.624
20	.965	.999	1.037	1.081	1.131	1.188	1.255	1.334	1.427	1.538
25	.972	1.003	1.038	1.078	1.123	1.175	1.235	1.305	1.385	1.479
30	.978	1.006	1.038	1.074	1.115	1.162	1.216	1.278	1.350	1.433
35	.983	1.008	1.037	1.069	1.107	1.149	1.198	1.253	1.317	1.391
40	.986	1.009	1.035	1.064	1.098	1.136	1.801	1.230	1.287	1.353
45	.989	1.010	1.033	1.059	1.090	1.124	1.164	1.208	1.259	1.318
50	.992	1.010	1.030	1.054	1.081	1.112	1.148	1.188	1.234	1.286
55	.994	1.010	1.028	1.049	1.073	1.101	1.132	1.169	1.210	1.256
60	.996	1.009	1.025	1.043	1.065	1.090	1.118	1.150	1.187	1.229
65	.997	1.008	1.022	1.038	1.057	1.079	1.104	1.132	1.165	1.203
70	.998	1.007	1.019	1.032	1.049	1.068	1.090	1.116	1.145	1.178
75	.999	1.006	1.015	1.027	1.041	1.057	1.077	1.099	1.125	1.154
80	1.000	1.005	1.012	1.021	1.033	1.047	1.064	1.083	1.106	1.132
85	1.000	1.003	1.008	1.015	1.025	1.036	1.051	1.068	1.087	1.110
90	1.000	1.001	1.004	1.009	1.017	1.026	1.038	1.052	1.069	1.089
95	1.000	.999	1.000	1.003	1.008	1.016	1.025	1.037	1.052	1.069
100	1.000	.997	.996	.997	1.000	1.005	1.013	1.022	1.034	1.049
105	.999	.994	.991	.990	.992	.995	1.000	1.007	1.017	1.029
110	.998	.991	.986	.984	.983	.984	.987	.993	1.000	1.010
115	.997	.988	.981	.977	.974	.973	.974	.978	.983	.990
120	.996	.985	.976	.969	.965	.962	.961	.963	.966	.971
125	.994	.981	.970	.961	.955	.950	.948	.947	.948	.952
130	.992	.977	.964	.953	.945	.938	.934	.931	.931	.932
135	.989	.972	.957	.944	.934	.926	.920	.915	.913	.912
140	.986	.967	.950	.935	.923	.913	.905	.898	.894	.892
145	.983	.961	.941	.925	.911	.899	.889	.881	.875	.871
150	.978	.954	.932	.916	.897	.884	.872	.862	.855	.849
155	.972	.945	.922	.901	.883	.867	.854	.843	.833	.826
160	.965	.936	.910	.887	.867	.849	.834	.821	.810	.801
165	.956	.924	.895	.870	.848	.829	.812	.798	.785	.775
170	.943	.907	.876	.850	.826	.805	.787	.771	.757	.745
175	.950	.903	.862	.827	.798	.774	.753	.737	.722	.709
180	.993	.938	.889	.846	.808	.774	.744	.717	.694	.673

TABLE VII.—COORDINATES θ AND $r/(1.078A)$ OF THE BOUNDARY OF THE HOLLOW FOR VARIOUS λ, EXACT SOLUTION FOR TWO-DIMENSIONAL PROBLEM—Concluded

$$\varphi = \frac{\pi}{2}$$

θ, deg	λ, deg									
	0	5	10	15	20	25	30	35	40	45
0	0.993	1.056	1.127	1.210	1.304	1.415	1.545	1.699	1.885	2.113
5	1.063	1.133	1.214	1.307	1.415	1.543	1.695	1.878	2.103	2.383
10	1.153	1.231	1.322	1.428	1.554	1.703	1.883	2.104	2.380	2.725
15	1.259	1.348	1.452	1.575	1.721	1.899	2.116	2.388	2.725	3.192
20	1.382	1.483	1.604	1.749	1.923	2.138	2.407	2.737	3.205	3.978
25	1.521	1.640	1.783	1.956	2.169	2.435	2.760	3.232	4.006	5.258
30	1.681	1.823	1.995	2.207	2.472	2.792	3.271	4.049	5.296	7.207
35	1.867	2.038	2.249	2.515	2.833	3.320	4.107	5.353	7.247	
40	2.085	2.296	2.559	2.881	3.379	4.177	5.425	7.305		
45	2.345	2.605	2.934	3.446	4.257	5.511	7.380			
50	2.654	2.992	3.518	4.344	5.606	7.468				
55	3.052	3.594	4.436	5.709	7.567					
60	3.672	4.532	5.816	7.672						8.685
65	4.627	5.925	7.783						8.656	6.664
70	6.034	7.895						8.613	6.643	5.188
75	8.006						8.555	6.607	5.170	4.155
80						8.486	6.556	5.138	4.137	3.465
85					8.405	6.493	5.093	4.108	3.446	3.018
90				8.315	6.418	5.037	4.068	3.417	2.997	2.708
95			8.217	6.332	4.970	4.018	3.381	2.968	2.685	2.439
100		8.113	6.238	4.893	3.960	3.337	2.934	2.657	2.415	2.216
105	8.006	6.138	4.809	3.894	3.287	2.894	2.622	2.386	2.191	2.028
110	6.034	4.720	3.824	3.232	2.851	2.584	2.352	2.161	2.001	1.866
115	4.627	3.748	3.174	2.804	2.541	2.313	2.126	1.970	1.838	1.725
120	3.672	3.113	2.754	2.494	2.271	2.088	1.936	1.806	1.695	1.600
125	3.052	2.704	2.446	2.227	2.047	1.897	1.771	1.663	1.569	1.488
130	2.654	2.395	2.180	2.003	1.856	1.732	1.626	1.535	1.456	1.387
135	2.345	2.132	1.958	1.813	1.691	1.587	1.498	1.421	1.354	1.295
140	2.085	1.912	1.769	1.648	1.546	1.459	1.383	1.318	1.260	1.210
145	1.867	1.724	1.605	1.504	1.418	1.344	1.279	1.223	1.174	1.131
150	1.681	1.562	1.462	1.376	1.302	1.239	1.184	1.135	1.093	1.056
155	1.521	1.420	1.334	1.261	1.198	1.143	1.095	1.054	1.017	.985
160	1.382	1.295	1.221	1.157	1.102	1.054	1.013	.977	.945	.918
165	1.259	1.184	1.118	1.062	1.014	.971	.935	.903	.876	.852
170	1.153	1.086	1.027	.977	.933	.895	.862	.833	.809	.788
175	1.063	1.002	.949	.902	.861	.826	.795	.768	.745	.725
180	.993	.938	.889	.846	.808	.774	.744	.717	.694	.673

TABLE VIII.—COORDINATES θ_N AND $r_N/(1.078A)$ OF NEUTRAL POINTS FOR VARIOUS λ, EXACT SOLUTION FOR TWO-DIMENSIONAL PROBLEM

	λ, deg									
	0	5	10	15	20	25	30	35	40	45
θ_{N_U}, deg	11.06	12.42	13.81	15.24	16.68	18.12	19.55	20.97	22.34	23.65
ρ_{2N_U}	0.945	.9875	1.033	1.082	1.136	1.194	1.257	1.328	1.406	1.493
θ_{N_L}, deg	168.94	170.25	171.50	172.69	173.80	174.83	175.77	176.62	177.36	178.01
ρ_{2N_L}	0.945	0.906	0.870	0.836	0.804	0.775	0.748	0.723	0.700	0.680